Do environmental justice policies narrow inequality?*

Danae Hernandez-Cortes, Kyle Meng, Chris Timmins & Paige Weber

January 2025
PRELIMINARY DRAFT

Abstract

How does improving the local environment impact welfare inequality? This paper combines an equilibrium location sorting model with a novel reduced-form estimator of pollution's general equilibrium effects to quantify the welfare disparity consequences of demographically-targeted environmental policies. We apply this framework to recent years in Chicago, using data on individual migration histories and air pollution, an atmospheric transport model, and a research design leveraging local air pollution changes from remotely-determined natural gas extraction. We find that targeted place-based policies designed to narrow environmental inequality can widen welfare inequality.

*Hernandez-Cortes: School of Sustainability and School for the Future of Innovation in Society, Arizona State University, Danae.Hernandez-Cortes@asu.edu, Meng: Bren School and Dept. of Economics, UC Santa Barbara and NBER, kmeng@bren.ucsb.edu, Timmins: Real Estate and Urban Land Economics Department at the Wisconsin School of Business ctimmins@wisc.edu Weber: Energy and Resources Group, UC Berkeley, paigeweber@berkeley.edu. The authors have no financial or other conflicts of interest to disclose.

1 Introduction

A growing literature documents systematic disparities in pollution exposure across locations where individuals of different race/ethnicity and socio-economic status reside.[1] Such pollution disparities have prompted calls for environmental justice policies – broadly, policies that explicitly clean up locations where minoritized individuals reside. However, it remains unclear how such targeted place-based environmental policies impact welfare inequality between individuals from minoritized and other groups (Depro, Timmins and O'Neil, 2015; Banzhaf, Ma and Timmins, 2019; Wang, 2021).

Consider a policy that improves local air quality. Rosen (1974)'s canonical economic model describing the sorting of households in locations with heterogeneous amenities predicts that improved air quality increases housing prices and rents. In this case, some individuals may relocate to find lower housing costs and subsequently not benefit from the environmental benefits at their former homes. Meanwhile, individuals with high value for air quality, or alternatively, high frictions to moving, may stay and enjoy the cleaner air provided by the policy, while paying more for housing.

Welfare changes across demographic groups depend not only on the change in the environment, but also on how resulting changes in housing prices and other amenities across locations induce migration patterns. Recent empirical studies document an expanding set of local amenities affected by local and nearby air quality; for example, education, crime, recreation[2], but do not link such impacts to welfare. A fully structural approach would explicitly model the endogeneity of each of these amenities within a welfare framework.[3] This must then be paired with separate identification strategies for estimating preferences of each amenity, along with the assumption that all relevant amenities are accounted for structurally

[1] These disparities are often referred to in the literature as an environmental justice gap (EJ gap). EJ gaps across many settings have been shown through case (Bullard, 2000; Bowen, 2002; Ringquist, 2005; Mohai, Pellow and Roberts, 2009*a*; Banzhaf, Ma and Timmins, 2019) and population-level (Tessum et al., 2019; Colmer et al., 2020; Currie, Voorheis and Walker, 2020) studies. See Cain et al. (2024) for a summary of the last 10 years of economics oriented research in environmental justice, and Mohai, Pellow and Roberts (2009*b*) provides a summary of earlier EJ research prior to that.

[2] The following provide empirical documentation of indirect amenity effects of pollution on education: (Currie et al., 2009; Persico, Figlio and Roth, 2020; Liu and Salvo, 2018); crime: (Bondy, Roth and Sager, 2020; Herrnstadt and Muehlegger, 2015); and recreation (Liu, Hanley and Campbell, 2020; Liang et al., 2020).

[3] For an example of this approach, see Diamond (2017).

and empirically.

This paper develops a hybrid framework for quantifying changes in welfare dispersion among renter households that live in locations that experience a cleaner environment. Our approach builds on a discrete location choice model to facilitate a welfare interpretation. Within this model, we develop a novel reduced-form approach to flexibly estimate the impact of local and non-local environmental improvements on welfare through both direct and indirect channels operating through changes in rental prices and endogenous amenities. Importantly, we need not assume the specific set of amenities affected by local and non-local environmental changes, nor recover amenity-specific structural preference parameters. We apply this framework to recent years in Chicago, using data on individual migration histories and air pollution, an atmospheric transport model, and a research design leveraging air pollution changes from remotely-determined natural gas extraction.

The goal of this paper is to understand whether inequality, as measured in terms of total welfare (expected utility), narrows or widens across different race groups following a clean-up of the local environment among renter households that initially live in that locality. In addition, because the stated outcome of interest in environmental justice policies is often pollution and not welfare, we will also ask how these policies impact pollution disparities accounting for general equilibrium effects. For our empirical application, we study the improvement in local air quality in the Chicago core-based statistical area (Chicago-Naperville-Elgin CBSA, Chicago CBSA thereafter) driven by quasi-random variation in the air pollution emissions intensity of electricity production – namely, a shift of electricity production from coal to gas following the advent of hydraulic fracking to access natural gas. Documenting the welfare dispersion effects of air quality improvements from the reduction of coal electricity production is not the main goal of this paper per se. Rather, we use this setting as a relevant and plausibly exogenous source of variation in a local environmental amenity. Specifically, we develop a formula instrument that quantifies how much and which census tracts experience air quality improvements by virtue of being downwind of coal plants that reduce electricity generation, attributable to shale gas propensity. Our identification strategy in this component of the paper leverages variation in the propensity of an area to be suitable for shale gas production, which is determined by geological characteristics.

We estimate the resulting air quality improvements explained by shale gas' role in shifting production from coal to gas, using an air pollution dispersal model to translate emissions to air quality. We study the welfare dispersion effects across race/ethnicity groups under the observed air quality improvements, as well as under simulated counterfactual approaches that yield the same total reduction in air pollution, though with different spatial patterns across Chicago.

To understand welfare impacts inclusive of residential re-sorting, this paper develops a household sorting model with a discrete location choice framework.[4] The model is similar to other residential location choice models, such as Bayer, Ferreira and McMillan (2007), and our welfare interpretation comes from Train (2009). We pair our sorting model with detailed bilateral migration data which allows us to estimate moving costs in line with the frontier of moving cost estimation in this literature. We include in the sorting model a control function approach from Davis, Gregory and Hartley (2023) to address possible omitted variable bias in the estimation of homophily preferences. Our model also incorporates indirect effects of one amenity improvement on other amenities. A robust line of research documents these indirect effects empirically for different environmental amenities (Currie et al., 2009; Persico, Figlio and Roth, 2020; Bondy, Roth and Sager, 2020; Liang et al., 2020; Stafford, 2015). In this paper we develop a new flexible approach to allow for these indirect effects without needing to precisely identify each one of them. In addition, we also allow the improvements in one location to impact the utility of living in nearby locations, which we call spillover effects. Our source of exogenous variation in air quality is estimated with a formula instrument involving shale gas propensity, pipeline density, and wind patterns.

We first estimate the impact of the air quality improvements that were observed in the Chicago CBSA over the period 2011–2018 on expected welfare changes by race. Then, we use our structural parameter estimates to simulate the effects of counterfactual spatial distributions of air quality improvements. Specifically, we simulate the following four cases: all locations improve by an equal percent; only locations with initial high shares of Black renters improve; only locations characterized as high priority by the Biden-Harris Adminis-

[4]See Kuminoff, Smith and Timmins (2013) for a review of the state of the literature on using sorting models and their use for policy analysis.

tration ("disadvantaged" tracts) improve; and, two fossil power plants in the Chicago CBSA shut down. For the first three simulations, aggregate pollution reductions are equivalent to observed reductions in the 2011–2018 period.

Across these simulations, we find that while targeting pollution improvements in certain locations can reduce pollution disparities, it can also widen welfare disparities, with white renters seeing larger welfare changes compared to Black renters. We compare our results to the results obtained in a partial equilibrium framework, which shuts down both re-sorting of renters and any changes in the prices and utility of indirectly effected amenities. We find that the welfare impacts of place-based clean-up on inequality are greatly overestimated in a partial equilibrium framework compared to our general equilibrium approach. This is a cautionary tale for cost-benefit analyses that use partial equilibrium approaches such as a marginal willingness-to-pay estimate to approximate the value of an amenity improvement. We also find that a partial equilibrium framework overestimates the impact of local air quality improvements on pollution disparities by shutting down possible re-sorting.

This paper contributes to the literature on hedonic housing market valuations, equilibrium sorting models used for policy analysis, and environmental justice. The existing literature has documented disparities in environmental amenities, finding that minority and low-income communities experience higher pollution on average (Tessum et al., 2021; Colmer et al., 2020; Currie, Voorheis and Walker, 2020). Some of the mechanisms behind these disparities are residential sorting (Depro, Timmins and O'Neil, 2015; Heblich, Trew and Zylberberg, 2021; Bakkensen and Ma, 2020), discriminatory behavior or policies (Christensen, Sarmiento-Barbieri and Timmins, 2022; Christensen and Timmins, 2022), and information about pollution sources (Hausman and Stolper, 2021; Wang et al., 2021). We advance this literature by pairing a source of exogenous variation in local air quality with an equilibrium sorting model. Further, we develop a novel technique for flexibly including endogenous amenities, that is, the indirect effects of changes in amenities on other amenities. Our modeling approach also captures spillovers of local amenity improvements to nearby locations. Our results are instructive for policymakers seeking to improve the local environment, advance equity-oriented goals, and avoid unintended consequences from policy that results from environmental gentrification channels and residential re-sorting. Overall, we elucidate

the connection between environmental policy and housing policy so that policy makers can better anticipate the outcomes of place-based environmental policy.

The rest of the paper proceeds as follows. Section 2 describes the model, Section 3 describes the data, Section 4 details the estimation method, Section 5 presents the results, and Section 6 concludes.

2 Model

In Section 2.1 we present a discrete choice model that is used to characterize equilibrium sorting outcomes. Section 2.2 presents a welfare metric that emerges from the modeling framework in Section 2.1, which facilitates our analysis of the relative welfare changes by race groups. Section 2.3 presents a new modeling approach for measuring the general equilibrium effects of an air quality improvement. This new methodology flexibly captures indirect effects of air quality improvements on other amenities, as well as spillovers of local amenity improvements to other locations.

2.1 Sorting Model

Residential location choices and equilibrium sorting outcomes are modeled as follows. Let t index years $t \in T = \{2011, ..., 2018\}$ and j index locations, which we define as census tracts. Renter households[5]—henceforth, households—are indexed by i. Households are grouped according to income type $\ell \in \{1, 2, 3, 4\}$ with $\ell = 1$ denoting the lowest income quantile and 4 denoting the highest. They are also grouped by race type r denoting Black, white, or other race. Households choose location j^* to rent at each time t by selecting the location that yields the highest utility U_{ijt} among J possible tracts. J denotes the set of tracts in a given market, which we define as a core-based statistical area (CBSA) plus an additional

[5]This paper is focused on renters, and we leave the plausibly dynamic decision problem of owner households, who make location decisions that involve future housing value, to future work. Table A1 shows that the percentage of renters who moved in the 2010-2018 period is 27.4% nationally and 30.8% in the Chicago CBSA, while the percentage of owners who moved is 7. 1% and 7. 9% nationally and in the Chicago CBSA, respectively.

outside option to move outside the CBSA or outside the market.[6] Each household's location choice satisfies the following:

$$\begin{aligned} j^* &= argmax_{j \in J}\{U_{ijt}\} \\ U_{ijt} &= V_{ijt} + \epsilon_{ijt} \\ V_{ijt} &= \delta^{\ell}_{jt} + \zeta^{\ell r} m_{it} + \psi^r S_{rjt} + \nu^r S^2_{rjt} + \chi^r a_{rj}, \end{aligned} \tag{1}$$

where m denotes a move across tracts, with $m = 1$ if $j_{t-1} \neq j_t$. S_r denotes the share of the tract that is the race of the renter i with ψ^r and ν^r denoting race specific parameters for the preferences of living in census tract with a large share of the population of their own race (homophily). a_r denotes amenities with race-specific preferences, captured in χ^r. Our empirical approach will assume these are unobserved. δ^{ℓ}_{jt} is the component of the utility that is specific to the location, time and income group – in other words, the baseline utility for all renters in location j at time t of the income group ℓ. This component of utility is modeled:

$$\delta^{\ell}_{jt} = \alpha^{\ell} p_{jt} + \rho^{\ell} x_{jt} + \gamma^{\ell}_j + \mu^{\ell}_t + \nu^{\ell} Q_{jt}, \tag{2}$$

where p denotes rent prices and x denotes air quality.[7] The corresponding sets of fixed effects α^{ℓ} and ρ^{ℓ} represent preferences for each, which can vary by income group. γ_j and μ_t denote location and year-specific determinants of location utility, respectively. Q_{jt} denotes a set of other location-by-income specific factors that impact utility — our empirical approach presumes that these are unobserved and potentially affected by air quality changes. More specifically, $E[x_{jt}Q_{jt}] \neq 0$ and $E[p_{jt}Q_{jt}] \neq 0$. The implications of this assumption are discussed below.

[6]The universe of households that we study, $i \in N$, includes all households living in the market of interest at $t = 2010$. Although we will estimate the model for the years 2011–2018, renter locations are needed one year prior to identifying who moved in the first year. Households that are present in the panel in 2010 but not in later years are assumed to have chosen the outside option, e.g., moved outside the CBSA. This assumption is problematic if a large share of those who leave the panel leave instead because they become unhoused.

[7]Our empirical estimation will allow for air quality to impact location utility non-linearly.

We note several features and assumptions in our model. First, note that the terms included in δ_{jt}^{ℓ} are indexed by ℓ but not r. We make this choice given the lack of theoretical motivation and sufficient empirical evidence that preferences for air quality and income structurally vary by race. Next, renters are myopic and make annual location choices. This modeling decision is motivated by the prevalence of yearlong leases and is supported by the year-to-year variation in air quality we exploit. This modeling choice, together with our subsequent estimation approach, requires that location utilities re-equilibrate to air quality changes annually. We relax this assumption in Appendix E where we estimate a long-difference version of this model and present the corresponding findings. Second, renters make choices based on the characteristics of the location in the concurrent year. This requires that renters have rational expectations about the current characteristics of the location year.[8]

Finally, we note that our modeling framework is consistent with empirical evidence documenting race-based discrimination in housing choice sets such as by Christensen, Sarmiento-Barbieri and Timmins (2022) and Christensen and Timmins (2022). These and related race-based frictions in moving are captured by race- and income-specific moving costs $\zeta^{\ell r}$, which we estimate with bilateral migration data.

2.2 Welfare

Using a logit discete choice framework, with the assumption that the unobserved term ϵ_{ijt} is drawn from an extreme value type-1 distribution, Train (2009) shows that $E[W_i] = \frac{1}{\alpha^{\ell}}\left[ln\left(\Sigma_{j=1}^{J} exp\{\widehat{V}_j\}\right)\right] + C$, where $\widehat{V}_j$ are constructed with the estimated parameters of the model, and C is an unknown constant. Now, consider two J-sized element vectors of air quality $\mathbf{x}_1$ and $\mathbf{x}_0$ in a given year. The following ratio compares changes in expected welfare across the these two states for Black (B) versus white (W) in a given income group:

[8]For an illustration for air quality, this implies that renters deciding where to live in 2011 have rational expectations about average annual air quality in 2011. Interannual changes in air quality would be included in utility when they are correlated with the overall average annual air quality. Related dimensions of annual air quality variation are discussed in Section 4.3 and Appendix B.

$$r_{BW=}\frac{E[\Delta W_{iB}]}{E[\Delta W_{iW}]} = \\ = \frac{\frac{1}{\alpha^{\ell}}\left[ln\Big(\Sigma_{j=1}^{J} exp\big\{\widehat{V}_{jB}(\mathbf{x_1})\big\}\Big) - ln\Big(\Sigma_{j=1}^{J} exp\big\{\widehat{V}_{jB}(\mathbf{x_0})\big\}\Big) - (C_B - C_B)\right]}{\frac{1}{\alpha^{\ell}}\left[ln\Big(\Sigma_{j=1}^{J} exp\big\{\widehat{V}_{jW}(\mathbf{x_1})\big\}\Big) - ln\Big(\Sigma_{j=1}^{J} exp\big\{\widehat{V}_{jW}(\mathbf{x_0})\big\}\Big) - (C_W - C_W)\right]}. \quad (3)$$

$\widehat{V}_{j\ell}(\cdot)$ are the estimated utilities specific to the location income group as a function of the air quality across all locations, including the effects of sorting and endogenous amenities on utility. The inclusion of the constants in the numerator and denominator is to make it explicit that while the logit framework does not allow us to compare levels of utility in any one state across income-race groups, we can compare changes in utility from one state to another across two groups of the same income type. The inclusion of the term $\frac{1}{\alpha^{\ell}}$ that cancels out of the equation is to demonstrate the benefits of this ratio as an object of interest: one can estimate this ratio without estimating the marginal utility of income, which is difficult to estimate without bias.

Denote the ratio in equation (3) r_{BW}. When the policy in x_1 improves welfare for both races compared to the the state x_0, the numerator and denominator are both positive. In this case, $r_{BW} > 1$ indicates that the policy is welfare narrowing, while $r_{BW} \in (0, 1)$ indicates that the policy are welfare widening, with $r_{BW} = 1$ indicating the relative welfare changes are equal. If the numerator and denominator are both negative, the policy reduces welfare for both race groups and $r_{BW} > 1$ indicates that the policy reduces welfare more for Black compared to white. If the numerator is negative (positive) and the denominator is positive (negative), $r_{BW} < 0$ and the value indicates the relative loss (gain) of welfare for Black compared to the gain (loss) for white.

2.3 General equilibrium effects of local air quality

In this section we present how we account for the fact that other amenities, Q_{jt}, may be impacted by changes in air quality. The motivation for including this channel comes from an expanding empirical literature documenting the effects of air quality improvements on other

amenities.[9] With this in mind, suppose that an improvement in air quality in one locality also increases the desirability of schools in that region due to the positive impact of air quality improvements on student learning. And perhaps the value of existing outdoor parks improved with air quality. Even if one could estimate or use previous literature's estimates of the impact of air quality on school and outdoor park quality, one could come up with an enumerable number of other plausible indirect effects for which empirical estimates and data are not available. A separate, but related issue with estimating the impact of air quality improvements on location utility regards spillovers across space. In the examples above, a higher quality school increases the location utility not only of the census tract the school is located in, but also in nearby tracts for households that have that school in their choice set. And a higher-quality outdoor park also benefits households outside of the park's own census tract, as households may travel across tracts to access it.

Our approach avoids trying to separately estimate each of these indirect effects—effects across amenities—and spillover effects—effects across space. We develop the following flexible approach to capturing the aggregate of each of these effects.[10] Our structural equation for the unobserved component of utility, equation (2), models δ_{jt}^{ℓ} as a function of rent prices, p_{jt}, and unobserved amenities, Q_{jt}, as well as location and time fixed effects. We decompose prices and unobserved amenities as:

$$\begin{aligned} p_{jt} &= \kappa_{P0} x_{jt} + \kappa_{P1} z_{jt} + \zeta_{Pjt} \\ Q_{jt} &= \kappa_{Q0} x_{jt} + \kappa_{Q1} z_{jt} + \zeta_{Qjt}. \end{aligned} \tag{4}$$

where z_{jt} denotes distance weighted air quality of neighboring locations and is modeled as $\sum_{k \neq j} s_{jk} x_{kt}$, where s_{jk} are spatial weights modeled as $s_{jk} = 1/d_{jk}$ with d_{jk} being the Euclidean distance between locations j and k. ζ_{Pjt} is an error term capturing all other deter-

[9] The following provide empirical documentation of indirect amenity effects of pollution on education: (Currie et al., 2009; Persico, Figlio and Roth, 2020; Liu and Salvo, 2018); crime: (Bondy, Roth and Sager, 2020; Herrnstadt and Muehlegger, 2015); and recreation (Liu, Hanley and Campbell, 2020; Liang et al., 2020).

[10] While we have not seen this approach used in other sorting models to handle endogenous amenities, a related technique is used in a working paper by Berry and Haile (2024) to address endogeneity in voting choices.

minants of housing rental price, and ζ_{Qjt} is an error term capturing all other determinants of other amenities. Implicit in eq. (4) is the assumption that rental prices in location j respond to own air quality via κ_0, and inverse-distance-weighted air quality from other locations via κ_1. This assumption is empirically tested with results provided in the appendix.

Inserting equation (4) into equation (2) yields:

$$\delta_{jt}^{\ell} = \underbrace{\left(\alpha^{\ell}\kappa_{P0} + \rho^{\ell} + \nu^{\ell}\kappa_{Q0}\right)}_{\beta_0^{\ell}} x_{jt} + \underbrace{\left(\alpha^{0}\kappa_{P1} + \nu^{\ell}\kappa_{q1}\right)}_{\beta_1^{\ell}} z_{jt} + \gamma_j + \mu_t + \underbrace{\alpha^{\ell}\zeta_{Pjt} + \nu^{\ell}\zeta_{jt}}_{\text{error}}. \qquad (5)$$

Thus, β_0^{ℓ} captures the aggregate effect of air quality on utility, inclusive of direct and indirect effects, e.g. the effects of air quality on other amenities. The usefulness of this formulation is that it allows us to sidestep separately estimating every indirect effect of air quality on other amenities. Rather, we will use exogenous changes in x_{jt} to estimate the aggregate effects of air quality on utility, including direct and any number of (including zero) indirect effects. This modeling approach does not require indirect effects to occur and the empirical estimation will identify their presence in this setting.

β_1^{ℓ} captures the aggregate impact of amenity improvements in locations $\neq j$ on utility in location j, which we refer to as spillover effects. These effects are again inclusive of direct and indirect effects and are assumed to be mediated though distance. This formulation allows improvements of an amenity in nearby tracts to improve own-tract utility, since households in nearby tracts can access or otherwise benefit from that amenity. As with the modeling of indirect effects, this modeling approach does not require spillover effects to occur, and the empirical estimates will reveal the size of the spillover effects. We call these parameters, $(\beta_0^{\ell}, \beta_1^{\ell})$, combined impact parameters—parameters which capture aggregate indirect effects and aggregate spillover effects of changes in local air quality. The empirical estimation will identify their magnitude in this setting by developing instruments for plausibly endogenous (x_{jt}, z_{jt}).

3 Data

This section discusses the data used to estimate both the residential sorting model and plausibly exogenous changes in air quality due to fracking. Data discussed in Sections 3.1 and 3.2 are used to estimate the sorting model and data discussed in Sections 3.3, 3.4, and 3.5 are used to estimate air quality changes driven by fracking.

3.1 Residential location data

We use the proprietary dataset InfoUSA Residential Historical Data Set from Data Axle (hereafter Data Axle) to observe household location decisions over time as well as household characteristics. These panel data are unique at the household–year level, allowing us to observe year to year bilateral migration decisions. Data Axle provides the household latitude and longitude, which we use to find the household's census tract of residence. We also use Data Axle's imputed inputs for household income, race, and status as renter or owner. We use the income variable to classify households into four income types to characterize each household's relative income types.

3.2 U.S. demographics, income, and rental prices

We use U.S. demographic, income, and rental data from the American Community Survey 5-year estimates (ACS 5-yr) for several supporting analyses. For the purposes of descriptive regressions and statistics, we use (real) rent prices from the ACS 5-yr, where we use each 5-year estimate as the rent price for the midyear, i.e., ACS 2009–2013 is used for rent prices in 2011. We match average rent values to migration data based on census tract identifiers. Table 1 panel (a) shows the average rent values alongside other demographics for the national average (column 1) and the Chicago CBSA (column 2) for our study period, 2010–2016. We also use income and demographic data from the ACS to construct our instrument for homophily discussed in Section 4.2.

Table 1: Descriptive statistics (census and Data Axle)

	(1)	(2)
	All census tracts	Chicago census tracts
Real rent	1038.584	1134.675
	(434.97)	(365.87)
Minority percent	0.356	0.477
	(0.31)	(0.33)
Black percent	0.133	0.214
	(0.22)	(0.33)
White percent	0.644	0.523
	(0.31)	(0.33)
Real median income	46289.506	47027.583
	(33404.30)	(36533.73)
Poverty percent	0.164	0.157
	(0.13)	(0.13)
Observations	586495	13219

NOTES: Descriptive statistics for the 2011–2018 period, nationally and for the Chicago CBSA. Panel (a) shows data from census obtained via IPUMS.

3.3 Electricity generating units data

We obtain data on electricity production and emissions (NO_x, SO_2) from the Clean Air Markets Division of the U.S. Environmental Protection Agency, which collects information on hourly data for electricity generating units over 25MW in capacity. We use these data to obtain annual emissions levels by electricity generating unit. We also use geographic information on units as well as smoke stack characteristics (height, velocity, temperature, and diameter) from the EIA Form 860 to model pollution dispersion. We follow the methods in Hernandez-Cortes, Meng and Weber (2023) to merge and process the electricity generating units data for use in the pollution dispersal model.

3.4 Shale gas propensity and natural gas pipelines

In Section 4.3 we present an instrumental variable approach for changes in ambient air quality. While the details of the identification argument are presented there, this section reviews the data used to construct the instrument. We use a measure of county-level fracking prospectivity score, which is used in Bartik et al. (2019) and originally constructed by Rystad Energy, a data provider and consulting firm. The score is developed to measure the potential productivity of different geographies using geological factors that determine

fracking potential. Because there are multiple shale plays in a county, we follow Bartik et al. (2019) and take maximum prospect score across all shale plays under a county. The county-level values of this score are mapped in panel (a) of Figure 1.[11]

The next data input for our instrument is the pre-shale network of natural gas pipelines. We use these data to connect shale gas propensity to changes in electricity production, as the degree to which a generator is impacted by fracking will depend on their proximity—in pipeline distance—to fracked gas. We use pipeline infrastructure data from the EIA's U.S. Energy Atlas and calculate the density of natural gas pipelines as pipeline area divided by county area. Panel (b) of Figure 1 shows the (normalized) share of county area with natural gas pipelines using the pipeline network in 2000, before the introduction of fracking.

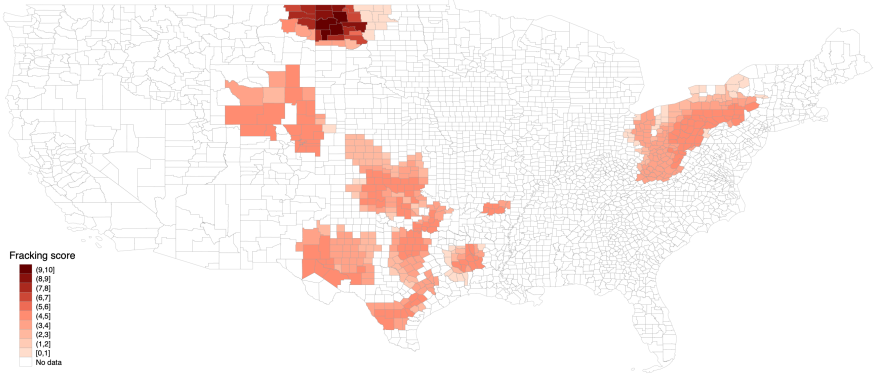
3.5 Air pollution data

We use two different measures of air pollution concentrations: (1) observed satellite data from Meng et al. (2019) which describes ambient pollution levels, e.g. air pollution from any source, and (2) pollution concentrations from electricity generating units using estimates from InMAP. InMAP is a pollution transport model based on electricity generating smoke stack unit characteristics and atmospheric and weather patterns developed by Tessum, Hill and Marshall (2017). We use InMAP's source-receptor matrix following Goodkind et al. (2019) to estimate how emissions from electricity generating units contribute to concentrations of $PM_{2.5}$ across a geographic grid of the contiguous U.S.. We then layer this spatial grid of pollution estimates onto U.S. census tracts to merge our $PM_{2.5}$ estimates with household location choices defined at the census tract level; additional details on this procedure are described in Hernandez-Cortes, Meng and Weber (2023). Figure A3 presents the data from these sources differenced over our study period, 2010–2016. Figure A3 panel (a) shows the observed changes in ambient $PM_{2.5}$ during 2010–2016 using the Meng et al. (2019) data, and Figure A3 panel (b) shows the changes in $PM_{2.5}$ concentrations from the electricity generating units in our sample generated by InMAP.

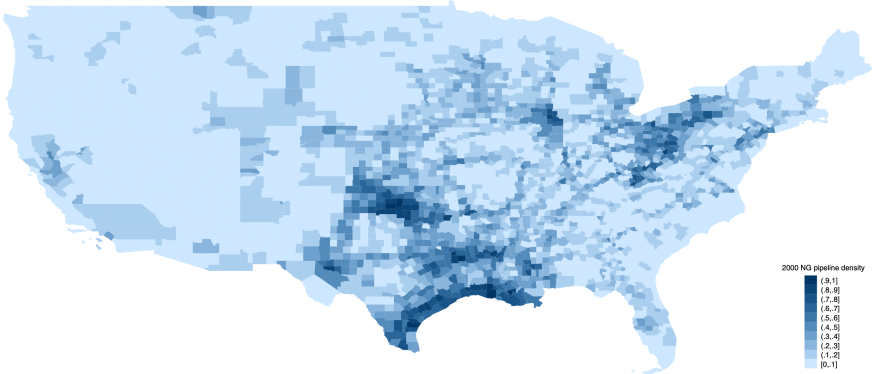
[11]Note that the geological factors that are inputs to the scores, as well as the functional forms, differ across shale plays so scores should not be compared across shale plays, but rather provide measures of county variation in fracking propensity within shale plays.

Figure 1: Maps of fracking propensity and natural gas pipeline density

(a) County-level prospect fracking score



(b) County-level 2000 natural gas pipeline density



NOTES: Panel (a) shows the county-level measure of shale gas propensity by fracking score, which constitutes variable (R_i) discussed in Section 4.3. Panel (b) shows the natural gas pipeline density by county across the contiguous U.S. and constitutes variable (G_i) discussed in Section 4.3.

4 Estimation

The following section discusses the estimation procedure, broadly grouped in two areas. Section 4.1 discusses the estimation of the parameters of the equilibrium sorting model. Section 4.3 discusses the estimation of the coefficients in equation (5), capturing the general equilibrium effects of air quality on utility.

4.1 Estimating parameters of the sorting model

The estimation of the parameters of the sorting model proceeds in two steps. First, a BLP-contraction algorithm is used to recover the unobserved location-time-income type-specific utilities, δ_{jt}^{ℓ} (Berry, Levinsohn and Pakes, 1995). Second, a nested likelihood maximization algorithm is used to estimate the unknown parameters for moving costs and homophily preferences. Details are provided below, where a will denote the iteration with respect to calculating the baseline utilities, δ_{jt}^{ℓ}, and q will denote the iteration with respect to calculating the remaining parameters.

Step (1). This step is a contraction mapping to recover unobserved utilities (δ_{jt}^{ℓ}) given an initial guess of $(\zeta^{\ell \cdot r}, \psi^{r}, \nu^{r}, \chi^{r})$. Assuming that ϵ_{ijt} are distributed i.i.d. Type I Extreme Value and given an initial guess for the parameters $(\zeta^{\ell \cdot r,q}, \psi^{r,q}, \nu^{r,q}, \chi^{r})$ and baseline utilities $\{\delta_{j}^{\ell,a,q}\}_{j=1}^{J}$, the probability that household i of income group ℓ chooses location j at time t is given by:

$$\pi_{i\in\ell j,t}^{a,q} = \frac{exp\big\{\delta_{jt}^{\ell,a,q} + \zeta^{\ell \cdot r} m_{it} + \psi^{r} S_{rjt} + \upsilon^{r} S_{rjt}^{2} + \chi^{r} a_{rj}\big\}}{\Sigma_{j=1}^{J}\big[exp\big\{\delta_{jt}^{\ell,a,q} + \zeta^{\ell \cdot r} m_{it} + \psi^{r} S_{rjt} + \upsilon^{r} S_{rjt}^{2} + \chi^{r} a_{rj}\big\}\big]} \tag{6}$$

From equation (6), the share of renters of income group ℓ living in location j at time t is given by:

$$\hat{\sigma}^{\ell,a,q} = \frac{1}{N}\sum_{i=1}^{N} \pi_{i\in\ell,jt}^{a,q} \tag{7}$$

Berry (1994) proves that the following iteration procedure will converge to the vector of δ_{jt}^{ℓ}'s

that equate observed to predicted shares, $\{\delta_{jt}^{\ell*,q}\}_{j=1}^{J}$ given the parameter vector $(\zeta^{\ell\cdot r,q}, \psi^{r,q}, \nu^{r,q}, \chi^{r})$:

$$\delta_{jt}^{\ell,a+1,q} = \delta_{jt}^{\ell,a,q} + (ln\ \sigma_{jt}^{\ell} - ln\ \hat{\sigma}_{jt}^{\ell,a,q}), \tag{8}$$

where σ_{jt}^{ℓ} denotes the observed share of individuals of type ℓ living in location j at time t. This procedure requires that one of the location-time-income group baseline utilities is normalized. We do this by setting $\delta_{j=1,t}^{\ell} = 0$, where $j = 1$ corresponds to the outside option. This normalization will allow us to estimate the expected welfare changes in 3, which compares welfare across races, but not across income types.

Step (2). Step (1) is nested inside a likelihood maximization algorithm. Given the parameter vector $(\zeta^{\ell\cdot r,q}, \psi^{r,q}, \upsilon^{r,q}, \chi^{r})$ and the corresponding vector of baseline utilities that equate predicted to actual shares, $\{\delta_{jt}^{\ell*,q}\}_{j=1}^{J}$, we can calculate the likelihood of the observed data:

$$L(\zeta^{\ell\cdot r,q}, \psi^{r,q}, \upsilon^{r,q}, \chi^{r}|x, p, \sigma, \theta) = \Pi_{t=1}^{T}\Pi_{n=1}^{N}\Pi_{j=1}^{J}\left[\pi_{ijt}^{*,q}\right]^{Y_{ijt}}, \tag{9}$$

where $Y_{ijt} = 1$ if renter i chooses j and $= 0$ otherwise. The maximization routine determines new values of $(\zeta^{\ell\cdot r,a}, \psi^{r,a}, \upsilon^{r,a}, \chi^{r})$ along with the corresponding values of $\left\{\delta_{jt}^{\ell*,q+1}\right\}_{j=1}^{J}$ to increase the likelihood expression until it is maximized as: $\{\zeta^{\ell\cdot r*}, \psi^{r*}, \upsilon^{r*}, \chi^{r*}\{\delta_{jt}^{\ell*}\}_{j=1}^{J}\}$.

Once $\{\delta_{jt}^{*}\}_{j=1}^{J}$ is recovered, the next step is to regress these estimated objects on exogenous changes to air quality, discussed below. We will use the set of recovered parameters to construct equation (3) to make welfare change comparison across observed and counterfactual air quality states.

4.2 Control function for homophily

The exposition of V_{ijt} in equation (1) includes the term $\chi^{r}a_{rj}$ which we mention is assumed unobserved. a_{rj} represents amenities with race-specific preferences and χ^{r} represents those race-specific preference parameters. Absent this term, these amenities and preferences would

be reflected in our estimates of homophily preferences, ψ and ν. This would not introduce a problem for our construction of welfare dispersion in the observed state. However, it presents an issue when considering counterfactual sorting equilibriums. Without pulling out amenities with race-specific preferences, we would likely be over-estimating the role of homophily.

To address this, we follow the approach in Davis, Gregory and Hartley (2023), which essentially constructs a control function for homophily. To implement the approach, we construct observed shares by narrow demographic group definition (e.g. age by race by income) across the U.S. to estimate conditional choice probabilities of living in census tracts by within CBSA income percentiles. Then, we regress observed shares in Chicago by those same sub-groups on the constructed predicted shares based on sorting patterns across the US. We interpret the residual of this regression as including amenities with race-specific preferences in Chicago, and include this residual as a_r in our sorting model.

4.3 Identification of air quality impacts on utility

Overview of approach. This section discusses our approach to causally identify the impact of cleaner air on a location's utility. Our approach is motivated by the fact that variation in air quality is potentially correlated with unobserved factors impacting utility. Specifically, x_{jt} and z_{jt} in equation (5) may be correlated with the error term. To address this, we leverage a plausibly exogenous source of variation in air quality—changes in air quality from the advent of horizontal drilling and hydraulic fracturing to access natural gas. Fracking also led to a number of local amenity impacts for the communities near fracked wells, some of which are empirically documented in Bartik et al. (2019) and Jacobsen (2019). Our empirical strategy does not make any assumptions that are inconsistent with this empirical finding.

While horizontal drilling and hydraulic fracking as (separate) techniques to access oil and gas have been around for many years, their use together to access crude oil and natural gas in the U.S. started growing in the early 2000s, taking off by the end of the decade. By October 2011, well footage drilled by these new techniques in the U.S. had surpassed all other drilling approaches. These techniques involve drilling a well first vertically, and then extending it horizontally. The fracturing part comes after the well is drilled. In this step a liquid under high pressure is forced against a rock formation until it fractures. The fluid,

which contains small, solid particles, expands the fractures, allowing crude oil or gas to be accessed more easily (U.S. EIA, 2018). Though these techniques, which we will collectively refer to as fracking, are more expensive in terms of capital costs compared to conventional drilling techniques, their impact on increasing supply of crude oil and natural gas has ultimately decreased the prices of these energy sources. The decrease in the the price of natural gas reduced the cost natural gas generated electricity (Hausman and Kellogg, 2015). As a result, electricity generation from coal generating units fell while electricity from natural gas generating units increased, with natural gas surpassing coal electricity generation in the U.S. in 2016 (U.S. EIA, 2017). Since natural gas generated electricity is less pollution intensive, fracking resulted in improvements in air quality. The level of air quality improvement will vary spatially, based on the spatial distribution of gas and coal plants and which generators have access to fracked-gas. We will use this feature of the empirical setting to improve the relevance of our instrument, bringing in the density of the U.S. natural gas pipeline network.

In general, changes in air quality attributed to the electricity sector are a function of both changes in emissions from electricity generating units—e.g. sources of pollution—and the wind patterns connecting those emissions changes to households receiving the pollution—e.g. receptors of pollution. We use the InMAP source receptor matrix to estimate the impact of emissions from electricity generating units on concentrations of pollution at receptor locations. InMAP is a model of pollution transport and thus includes measurement error. For example, its model of pollution transport uses average annual wind speeds as of year 2005, which means averages of seasonal trends in wind and may be outdated to the extent that average annual wind speeds and directions have changed in our study period. Our estimation is at the annual level, so averaging over seasonal outcomes is not a problem.

To the extent that wind speeds and directions have changed in the period 2011—2018 compared to 2005, that would introduce additional measurement error in the construction of our instrument. However, that error is unlikely to violate our exclusion restriction. It would present a problem for our exclusion restriction if changes in wind speed and direction created tract-by-year changes in pollution that were correlated with tract-by-year components of the error term in equation 5. Given changes in wind are due to weather and climate related factors, this is unlikely to be the case. The wind patterns introduced via InMAP will thus

provide another source of exogenous variation in our identification strategy, in addition to air pollution changes explained by shale gas prospectivity and pipeline network.

Below we discuss in detail our identification strategy to construct instruments for (x_{jt}, z_{jt}) that are uncorrelated with the error term in equation (5). We first construct fracking-induced predicted emissions from electricity generating units. The predicted emissions leverage the exogenous variation in shale gas prospect scores across counties in the U.S. The predictions are improved, e.g. relevance of the instrument increased, by incorporating natural gas pipeline density in the U.S. in the year 2000, i.e. before the widespread use of fracking techniques. Then, we use a pollution dispersal model to convert these predicted emission changes to predicted changes in air quality.

Isolating exogenous changes in emissions from generating units. In this estimation task, we isolate the changes in electricity generating unit (EGU) emissions that are due to exogenous variation in the spatial distribution of shale gas supply, modulated by pipeline density. Following Bartik et al. (2019), denote R_i as the fracking prospect score for county i, which is constructed using geological factors that determine fracking potential. Because there are multiple shale plays in a county, we follow Bartik et al. (2019) and take maximum prospect score across all shale plays under a county.[12] The availability of shale natural gas should affect electricity output in counties not overlying a shale play. The degree those counties are affected by shale gas exploration depends on the pre-shale network of natural gas pipelines.[13] Denote county-level natural gas pipeline density in 2000 as G_i.

For each EGU g in county i, we define potential fracking supply as $S_g = R_g * G_i$ where R_g is the prospective fracking score for the nearest county j to EGU g by Euclidean distance with a positive prospective fracking score, or $R_g = R_{i^*}$ where $i^* = min_{i \in R_i > 0} |g - i|$. Panel (a) of Figure A8 shows S_g for every EGU that operated between 2000–2018. Note that S_g jointly weights proximity to a natural gas shale play and pre-fracking natural gas pipeline availability. For example, whereas Ohio and South Dakota are similarly close to natural gas plays (the Marcellus and Bakken, respectively), the greater density of natural gas pipelines in 2000 in Ohio generates a higher potential fracking supply than in South Dakota. This is

[12]The county-level values for R_i is mapped in panel (a) of Figure 1.

[13]Panel (b) of Figure 1 shows the (normalized) share of county area with natural gas pipelines using the pipeline network in 2000, before the introduction of fracking.

consistent with observed changes in natural gas input prices for natural gas EGUs from EIA Form-923 data. As panel (b) of Figure A8 shows, the 2008–2018 drop in natural gas input prices is much larger near the Marcellus formation than near the Bakken formation.

Next, define h_{gt} as an event time variable whereby the value zero indicates the last year before fracking began in nearest county i^*. Let E^p_{gt} denote emissions of primary pollutant $p \in \{NO_x, SO_2, PM_{2.5}\}$ from EGU g in year t. Further let each EGU g be characterized by fossil fuel $f \in \{coal, gas, oil\}$. We estimate the following event-study regression specification:

$$asinh(E^p_{gt}) = \sum_{\substack{-4 \leq \tau \leq 10 \\ \tau \neq 0}} \kappa^{\text{gas}}_{p,\tau}[\mathbf{1}(\tau = h_{gt}) \times \mathbf{1}(f = \text{gas}) \times S_g] + \sum_{\substack{-4 \leq \tau \leq 10 \\ \tau \neq 0}} \kappa^{\text{coal}}_{p,\tau}[\mathbf{1}(\tau = h_{gt}) \times \mathbf{1}(f = \text{coal}) \times S_g] + \psi_g + \vartheta_{ot} + \nu^p_{gt}$$

where ψ_g are EGU-level fixed effects. The vector of dummy variables ϑ_{ot} includes power plant-by-year and event time fixed effects. The error term ν^p_{gt} is clustered at the county level to account for arbitrary forms of heteroskedascity for EGUs within a county and serial correlation within an EGU over time. Our coefficients of interest are $\kappa^{\text{gas}}_{p,\tau}$ and $\kappa^{\text{coal}}_{p,\tau}$. When event time $\tau > 0$, this coefficient indicates the annual percentage point change in pollutant p emissions for coal and natural gas EGUs relative to oil EGUs after fracking becomes locally available. The coefficients when event time $\tau < 0$ provide an indirect test for pre-trends. Figure 2 plots estimates of coefficients $\kappa^{\text{gas}}_{p,\tau}$ (left panel) and $\kappa^{\text{coal}}_{p,\tau}$ (right panel) for each of the three primary pollutants (down rows).

Equation (10) is the fully-flexible event study specification. Guided by the functional form shown in Figure 2, we further estimate a more parsimonious version using a linear trend break model. Specifically, we estimate:

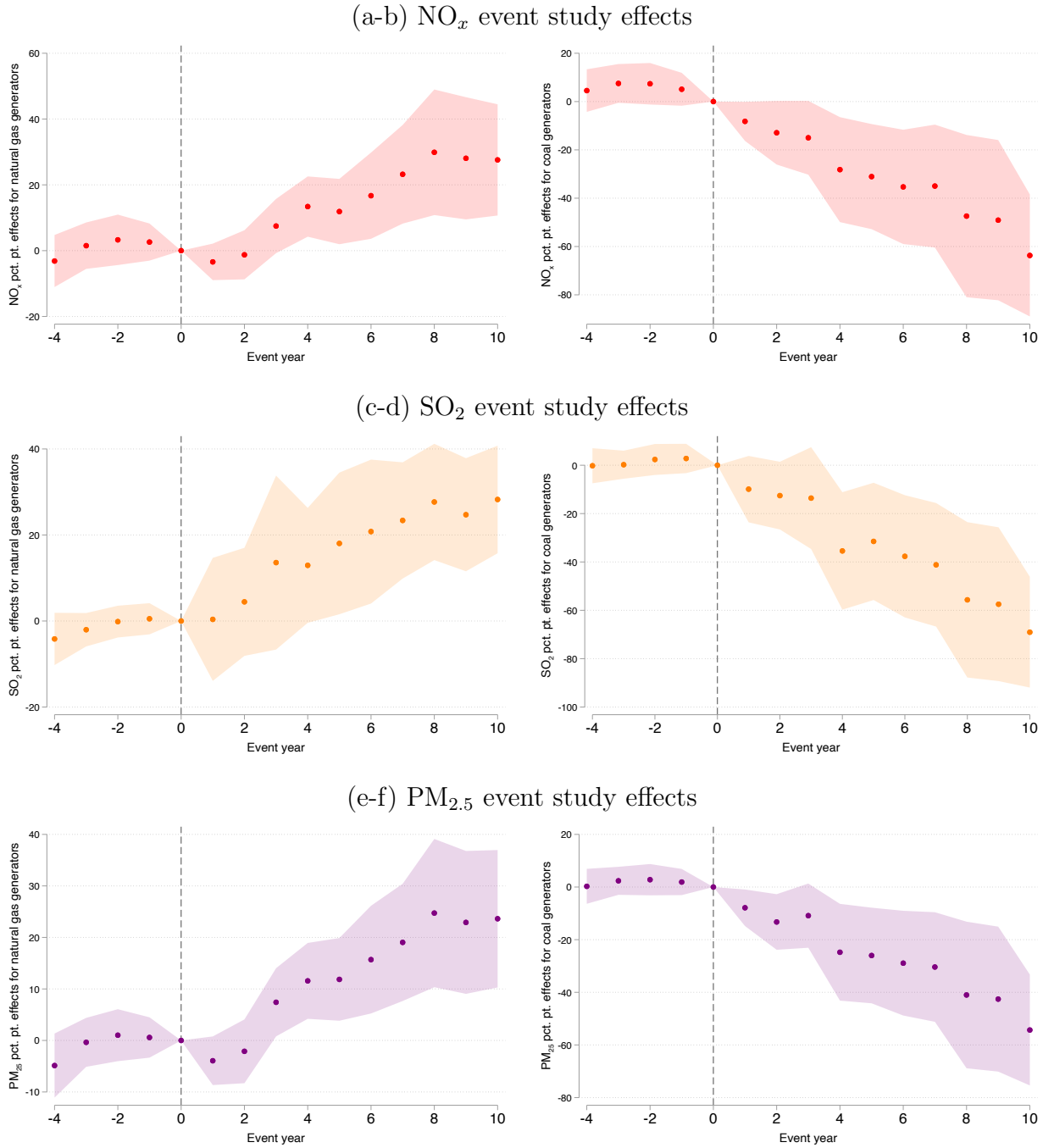
$$
\begin{aligned}
asinh(E^{pgt}) =& \beta^{\text{gas}}_{p,1}[h_{gt} \times \mathbf{1}(f = \text{gas}) \times S_g] + \beta^{\text{gas}}_{p,2}[h_{gt} \times \mathbf{1}(h_{gt} > 0) \times \mathbf{1}(f = \text{gas}) \times S_g] + \\
& \beta^{\text{gas}}_{p,3}[\mathbf{1}(h_{gt} > 0) \times \mathbf{1}(f = \text{gas}) \times S_g] + \\
& \beta^{\text{gas}}_{p,1}[h_{gt} \times \mathbf{1}(f = \text{gas}) \times S_g] + \beta^{\text{gas}}_{p,2}[h_{gt} \times \mathbf{1}(h_{gt} > 0) \times \mathbf{1}(f = \text{gas}) \times S_g] + \\
& \beta^{\text{gas}}_{p,3}[\mathbf{1}(h_{gt} > 0) \times \mathbf{1}(f = \text{gas}) \times S_g] + \\
& \psi_g + \vartheta_{ot} + \nu_{pgt},
\end{aligned}
$$

where our parameter of interests are now $\beta^{\text{gas}}_{p,2}$ and $\beta^{\text{coal}}_{p,2}$, which test whether emissions of pollutant p for natural gas and coal EGUs exhibit trend breaks after the introduction of local fracking. Table A3 shows that there are statistically significant trend breaks.

For each EGU, we generate predicted emission changes $\Delta\widehat{E}^{p}_{gt}$ due to the introduction of fracking. Specifically, letting E^{op}_{g} denote the observed emissions of pollutant p when event time is zero, $\Delta\widehat{E}^{p}_{gt} = E^{op}_{g}[\widehat{\beta}^{\text{gas}}_{p,2} * h_{gt} * S_g + \widehat{\beta}^{\text{gas}}_{p,3} + 1]$ for a gas EGU and $\Delta\widehat{E}^{p}_{gt} = E^{op}_{g}[\widehat{\beta}^{\text{coal}}_{p,2} * h_{gt} * S_g + \widehat{\beta}^{\text{coal}}_{p,3} + 1]$ for a coal EGU. Predicted emissions change may exceed the maximum within sample emissions for a given EGU. To avoid this over- or under-prediction, we replace $\Delta\widehat{E}^{p}_{gt}$ if its absolute value exceeds that of the maximum observed sample emissions value for that EGU. Panel (a) of Figure 3 plots 2010–2016 NO_x predicted emissions for coal EGUs. As a comparison, panel (b) of Figure 3 shows the observed NO_x change from coal EGUs during 2010–2016. Panels (c) and (d) of Figure 3 shows predicted and observed NO_x changes for natural gas EGUs. The mechanism generating these results is that shale gas propensity modulated by pipeline availability provides access to natural gas. For this to be true, gas EGUs with a large S_g would also have lower natural gas prices. We study this by generating the same event study figure with natural gas prices from EIA-923 as the outcome. Figure A2 which shows suggestive evidence of lower generator-level natural gas prices following the event year.

Converting emissions to air quality. In this estimation step we convert predicted EGU-level emissions generated from the procedure above, $\Delta\widehat{E}^{p}gt$, to total $PM_{2.5}$ concentrations for a census tract j, $\Delta\widehat{X}_{jt}$, which equals $\sum_p \sum_g w^{p}_{gj}\Delta\widehat{E}^{p}_{gt}$, where w^{p}_{gj} are elements from the InMAP source-receptor matrix converting emissions of pollutant p from generator g to

Figure 2: Effects of fracking on emissions and pollution from the electricity sector



NOTES: These figures plot the estimates from event study regression in equation (10), with alternative dependent variables—NO$_x$, SO$_2$, and PM$_{2.5}$. The figures in the left column—(a), (c), (e)—show the impacts among natural gas generators. The figures in the right column—(b), (d), (f)—show the impacts among coal generators.

census tract j. Figure 3 shows the 2010–2016 total predicted PM$_{2.5}$, $\Delta\widehat{X}_{jt}$. Our predicted

$PM_{2.5}$ concentrations show declines in the lower Midwest and the Southeast and also in the upper Midwest. Note the similarities between the spatial pattern of observed electricity sector pollution changes in Figure A3 panel (b) and those in Figure 3 – a regression between the two data series has an R^2 of 0.84. However, Figure 3 shows that there is not much observed coal decline in the upper Midwest and thus electricity may not have played a role in the clean up of the upper Midwest. This analysis motivates our choice of the Chicago CBSA as our empirical setting for our study of location choice—a CBSA with among the most variation in air pollution explained by fracking. Because the variation is due to plausibly exogenous factors, choosing Chicago to study should not introduce selection bias. Rather, we focus on the Chicago CBSA as here fracking provided a natural experiment with plausibly large enough variation in a local amenity to meaningfully impact location utility.

Let $\mathbf{W}^p$ be the p-pollutant source-receptor matrix (SRM), where element w^p_{gj} indicates the amount of secondary $PM_{2.5}$ pollution (in $\mu g/m^3$) received by census tract j from a one unit emission of primary pollutant p from EGU g. Total secondary $PM_{2.5}$ concentration (in $\mu g/m^3$) in location j and year t is then the product of a facility's p predicted emissions, $\widehat{E}^p_{gt}$, and its conversion to $PM_{2.5}$ concentrations in location i, summed over all facilities and pollutants. Denote that as $\widehat{X}_{jt} = \sum_p \sum_g w^p_{gj} \widehat{E}^p_{gt}$.

Next, recall the housing prices decomposition in equation (4). We instrument for x_{jt} and x_{jt} with the following two first stage regressions:

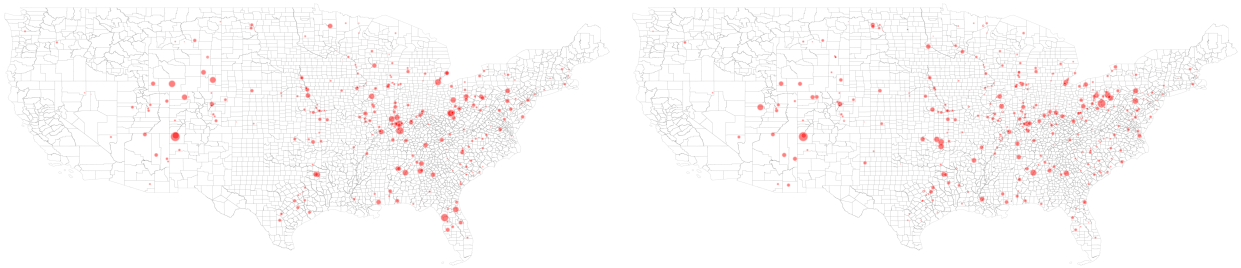
$$x_{jt} = \phi_{11} \widehat{X}_{jt} + \phi_{12} \widehat{Z}_{jt} + \varsigma_{1jt} \tag{10}$$

$$z_{jt} = \phi_{21} \widehat{X}_{jt} + \phi_{22} \widehat{Z}_{jt} + \varsigma_{1jt}, \tag{11}$$

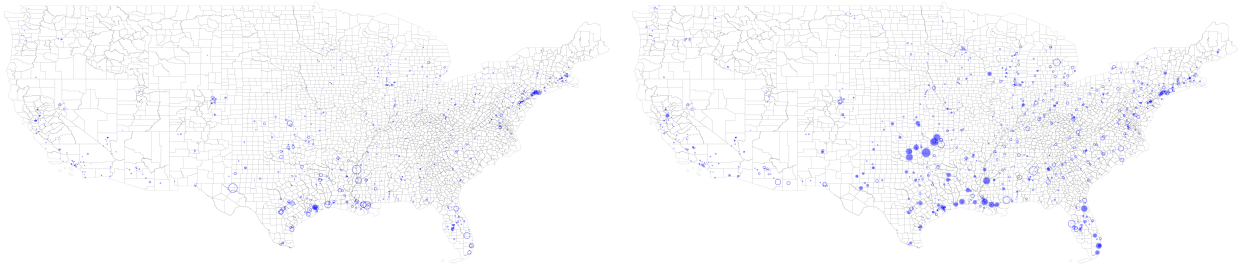
where $\widehat{Z}_{jt} = \sum_{k \neq j} s_{jk} \widehat{X}_{kt}$ is the distance-weighted fracking-induced air quality in locations $k \neq j$. In doing so, the reduced-form coefficients β^ℓ_0 and β^ℓ_1 capture all the direct and indirect effects of air quality on unobserved utility locally, as well as spillover effects that exhibit a distance gradient.

To conclude our argument that our instruments are valid in this setting, we demonstrate their relevance for predicting air quality with the first stage results with tract and year fixed

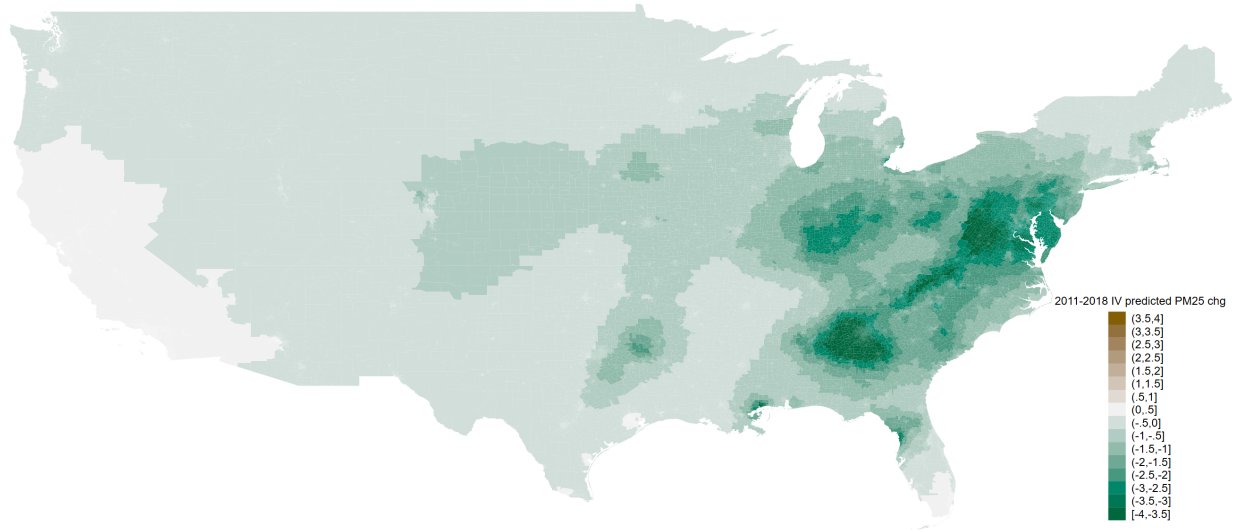
Figure 3: Effects of fracking on electricity emissions by fuel type and predicted $PM_{2.5}$



(a-b) Coal generators: predicted (a) and observed (b) NO_x change during 2011-2018



(c-d) Natural gas generators: predicted (c) and observed (d) NO_x change during 2011-2018



(e) Predicted $PM_{2.5}$ Changes, 2011–2018

NOTES: Panels (a) and (b) show the coal generators' predicted (panel a) and observed (panel b) NO_x change during 2010-2016. Panels (c) and (d) show the natural gas generators' predicted (panel c) and observed (panel d) NO_x change during 2010 and 2016. Solid circles represents decreases and hollow circles represents increases. Predicted pollution concentrations changes in the U.S. are based on the estimation procedure described in Section 4.3.

effects in Table A4 for our empirical setting of the Chicago CBSA. We can see that our instruments have predictive power on air quality, explaining almost a third of ambient air quality over 2011–2018. In terms of the exclusion restriction, we argue that the air pollution changes in census tract j explained by shale gas propensity modulated by pipeline density as of the year 2000 are unlikely to be correlated with other time-varying factors that impact utility which are also correlated with shale gas propensity and pipeline network. Note that the argument only needs to exclude time-varying factors, since our regression to estimate the combined impact parameters in equation (5) includes year and location fixed effects.

We will use our instrument to estimate equation (5) where the left hand side is replaced with $\widehat{\delta_{jt}^{\ell}}$, our estimates from the sorting model:

$$\widehat{\delta_{jt}^{\ell}} = f(x_{jt}, z_{jt}; \Theta) + \gamma_j^{\ell} + \mu_t^{\ell} + e_{jt\ell}. \tag{12}$$

To allow $\widehat{\delta_{jt}^{\ell}}$ to vary flexibly in own-tract and neighbor-tract air pollution, we estimate equation (12) non-parametrically with natural restricted cubic splines. We evaluate the performance of alternative non-parametric models, which vary in the number of knots used in the cubic spline: $\{3, 4, 5\}$; the number of 10km distance bands included in the set z of neighboring census tracts: $\{2, 3, 4, 5, 6\}$, and function used to measure neighboring tracts distance: euclidean, exponential, inverse hyperbolic sine, log. The AIC and BIC across models are shown in Table A5. We choose the model with the lowest AIC and BIC, which is a model with three knots, two neighbor distance bands, and an exponential function of distance.

5 Results

5.1 Parameter estimates

Table 2 shows our estimates of the parameters of the sorting model. Our model is in utility and not dollars, so these estimates are interpreted as such. The model includes a baseline moving cost estimate as well as race- and income- specific moving cost parameters which

modulate the baseline moving cost up or down. The excluded race and income group are the highest income white renters, so the baseline moving cost estimate applies to them. Black renters have higher moving costs in all income groups. White renters in the first and third income groups have higher moving costs as well, while white renters in the second lowest income group have lower moving costs. All income types in the non-Black and non-white race group have lower moving costs except in the second lowest income group. In the context of our model, our moving cost estimates will capture any and all frictions involved with moving to a new census tract in the Chicago CBSA, from the monetary costs associated to the move, to the psychological costs of leaving your home, or finding new employment. Racial discrimination in household choice sets, such as those documented in Christensen, Sarmiento-Barbieri and Timmins (2022), would arise in our model as an additional moving friction and would be embedded in these estimates.

Race-specific amenities are estimated to positively impact utility for all three race groups. Our estimates of the homophily parameters for all race groups indicate that the share of a census tract that is your own race, and the share squared, positively impact renter utility.

5.2 Observed and counterfactual changes in expected welfare

We estimate the welfare effects of four counterfactual simulations that improve local air quality in the Chicago CBSA. Each simulation starts with the unobserved location utilities and expected welfare estimated in 2011, models a change in air quality, and then estimates the changes in expected welfare changes from the air quality improvements compared to expected welfare in 2011. We use our estimates of the parameters of the sorting model in Table 2 together with our estimates of unobserved location-income-year utility, δ_{jt}^{ℓ}, to construct the ratio of expected welfare in equation (3).

The first simulation improves local air quality for each tract in the Chicago CBSA by an equal percentage. The percentage is selected such that the aggregate air quality improvement in this simulation corresponds to the aggregate air quality improvement observed in the CBSA from 2011 to 2018. We call this the *Improve All* simulation. The second simulation achieves the same aggregate pollution reduction, but targets air quality improvements in tracts in the Chicago CBSA with the top tercile of Black residents, which we call the *High*

Table 2: Sorting model parameter estimates

	Estimate	Std errors
ψ^r: black share	1.89	(–)
$\psi^{r,2}$: black share sq.	2.66	(–)
ψ^w: white share	2.30	(–)
$\psi^{w,2}$: white share sq.	1.05	(–)
ψ^w: non bl-wh share	0.94	(–)
$\psi^{w,3}$: non bl-wh sq.	1.73	(–)
$\chi^{r,1}$: race-specific amenity, black	1.54	(–)
$\chi^{r,2}$: race-specific amenity, white	1.13	(–)
$\chi^{r,3}$: race-specific amenity, non bl-wh	1.23	(–)
ζ Moving cost, baseline	-12.19	(–)
$\zeta^{b\cdot 1}$ Moving cost, black-w1 (lowest income)	1.03	(–)
$\zeta^{b\cdot 2}$ Moving cost, black-w2	2.06	(–)
$\zeta^{b\cdot 3}$ Moving cost, black-w3	0.50	(–)
$\zeta^{b\cdot 3}$ Moving cost, black-w4 (highest income)	1.92	(–)
$\zeta^{w\cdot 1}$: Moving cost, white-w1 (lowest income)	0.58	(–)
$\zeta^{w\cdot 2}$: Moving cost, white-w2	-0.98	(–)
$\zeta^{w\cdot 3}$: Moving cost, white-w3	1.07	(–)
$\zeta^{w\cdot 4}$: Moving cost, white-w4 (highest income)	NA	(–)
$\zeta^{w\cdot 1}$: Moving cost, non bl-wh-w1 (lowest income)	-0.31	(–)
$\zeta^{w\cdot 2}$: Moving cost, non bl-wh-w2	0.60	(–)
$\zeta^{w\cdot 3}$: Moving cost, non bl-wh-w3	-0.37	(–)
$\zeta^{w\cdot 4}$: Moving cost, non bl-wh-w4 (highest income)	-0.04	(–)

NOTES: Standard errors via bootstrap are forthcoming.

Black simulation. The third simulation achieves the same aggregate pollution reduction, but targets air quality improvements in the EJ 40 tracts, which are tracts identified in the Biden-Harris administration's Climate and Economic Justice Screening Tool as "disadvantaged" and prioritized for federal funding. We call this the *EJ 40* simulation. The fourth simulation shuts down two power plants in the Chicago CBSA, the Crawford and Fisk plants, located in the eastern region of the CBSA and operating on coal and diesel oil, respectively. The simulation reflects a practical policy approach—shutting down local pollution sources. The aggregate pollution from these two sources is below the aggregate reduction observed from 2011 to 2018, so this simulation's aggregate air quality improvement is not comparable to the other simulations. We call this the *Plant shutdown* scenario.

Panel (A) in Figure 4 shows the percent changes observed in air pollution concentrations between 2011 and 2018 and panel (B) in Figure 4 shows the changes in $\widehat{\delta_{jt}^{\ell}}$ due to the improvement of air quality in 2018. Figure 5 shows the air quality of the census tract in the Chicago CBSA under each of the counterfactual simulations. Figure 6 shows the estimated impacts of each simulated air quality on location utility. We construct the estimates of counterfactual location utility using our estimates $\widehat{\beta_0^{\ell}}$ and $\widehat{\beta_1^{\ell}}$ from equation (5) to estimate the $\widehat{\delta_{jt}^{\ell}}$s that result from different air quality simulations. As our goal is to allow unobserved location utility to vary with own-tract and neighbor-tract air quality very flexibly, we estimate equation (5) non-parametrically using cubic splines of own- and neighbor-tract air quality. Details on the nonparametric model chosen are provided in Appendix C. Then, we use our estimates of $\widehat{\delta_{jt}^{\ell}}$ in each of the counterfactual simulations and observed air quality in 2018 together with parameters estimates for homophily, moving costs, and amenity's with race-correlated preferences to construct the welfare change ratios in equation (3). This step necessarily involves an additional contraction mapping to find equilibrium race-shares in the new air quality states. The numerator we construct for the welfare change ratio in (3) is the difference between expected welfare in 2011 and welfare in the counterfactual air quality simulation for a given race in a given income type. The denominator is the same difference in expected welfare but for another race in the same income type.

To interpret the ratio r_{BW} correctly, we first establish the signs of the numerator and denominator. In all income types and scenarios the sign of the numerator is negative,

indicating a loss of welfare for Black renters. In all income types and scenarios, the sign of the denominator is positive, indicating welfare improvement for white renters. Thus, $r_{BW} < 0$ and the magnitude of the ratio indicates the relative welfare loss for Black renters compared to gain for white renters.

Figure 4: Observed air quality improvements in Chicago CBSA, 2011–2018

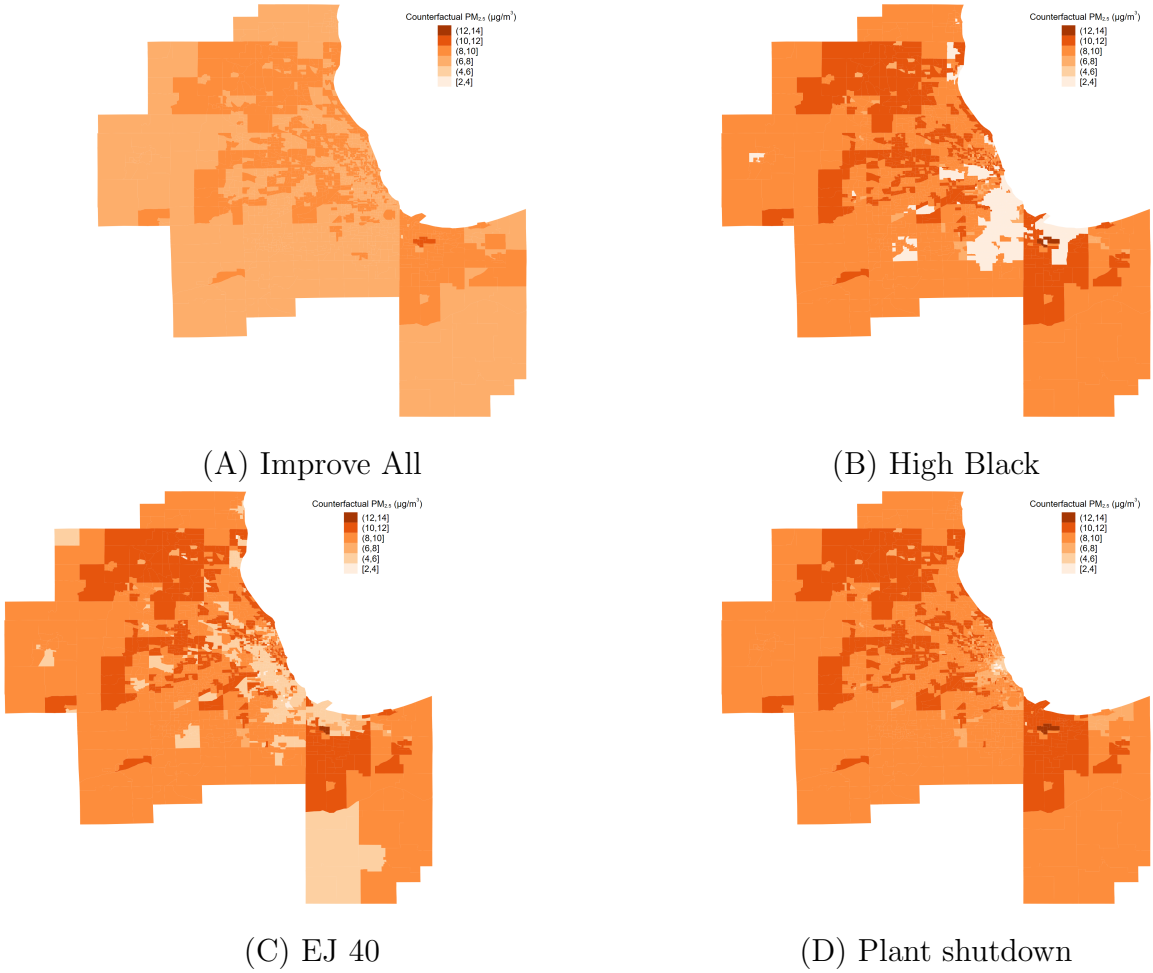


(A) Percent change in air quality from 2011 to 2018

(B) Changes in $\widehat{\delta_{jt}^{\ell}}$ due to 2018 air quality improvement

Figure 7 plots the ratios of expected welfare changes for Black versus white by each of the four income types in the observed and simulated policies. The shading of the purple circles is used to indicate the relative priority of EJ embedded in the policy, from the least priority in the *Improve All* simulation to the highest priority in the *High Black* simulation. This figure demonstrates three findings. First, on average across incomes, policies tend to widen race-based welfare inequality, with white renters on average experiencing welfare improvements, while Black renters experience loss in welfare. Second, the *Improve All* counterfactual is consistently more welfare widening than other counterfactuals, while the *High Black* counterfactual is the least widening. Third, the widening effect is greater for lower income types (1 and 2) compared to higher income types (3 and 4). Differences in effects between income groups stem from unique combined impact parameters $(\widehat{\beta_0^{\ell}}, \widehat{\beta_1^{\ell}})$–the impact of air quality on utility–for each income type, as well as the specific moving costs of income type (and race). Overall, these findings have dramatic implications for this class of placed-based EJ oriented policies—we find that these policies can widen overall welfare inequality, with worse outcomes in lower income groups.

Figure 5: Counterfactual air pollution



(A) Improve All (B) High Black

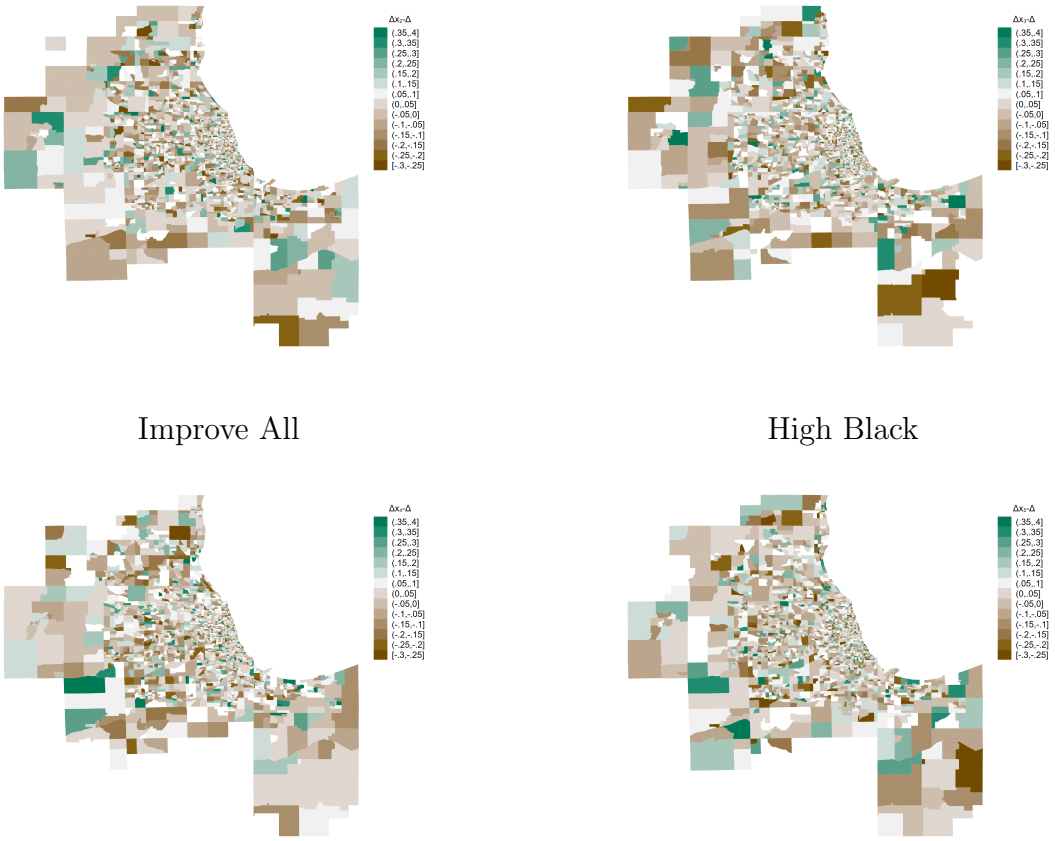
(C) EJ 40 (D) Plant shutdown

NOTES: This figure shows the air quality in concentrations of $PM_{2.5}$ across census tracts in the Chicago CBSA across the four counterfactual simulations.

5.3 Comparison partial equilibrium inequality measures

We compare our welfare ratio results to predictions that would emerge from a framework without sorting, or in other words, a partial equilibrium approach that does not account for the impacts of air quality changes on other inputs to welfare, such as housing costs and re-location decisions. To construct the welfare change ratios in a partial equilibrium approach, we use a comparable marginal willingess to pay (MWTP) for PM_{10} among renters from Grainger (2012). We assume that renters benefit from the simulated and 2018 air quality states based on this value, and then construct the ratio of those benefits by race. We compare those ratios to the ratios constructed above, which correspond to a general equilibrium framework. The results in this section represent average effects over income

Figure 6: Unobserved utility changes, $\widehat{\delta_{jt}}$



Improve All | High Black

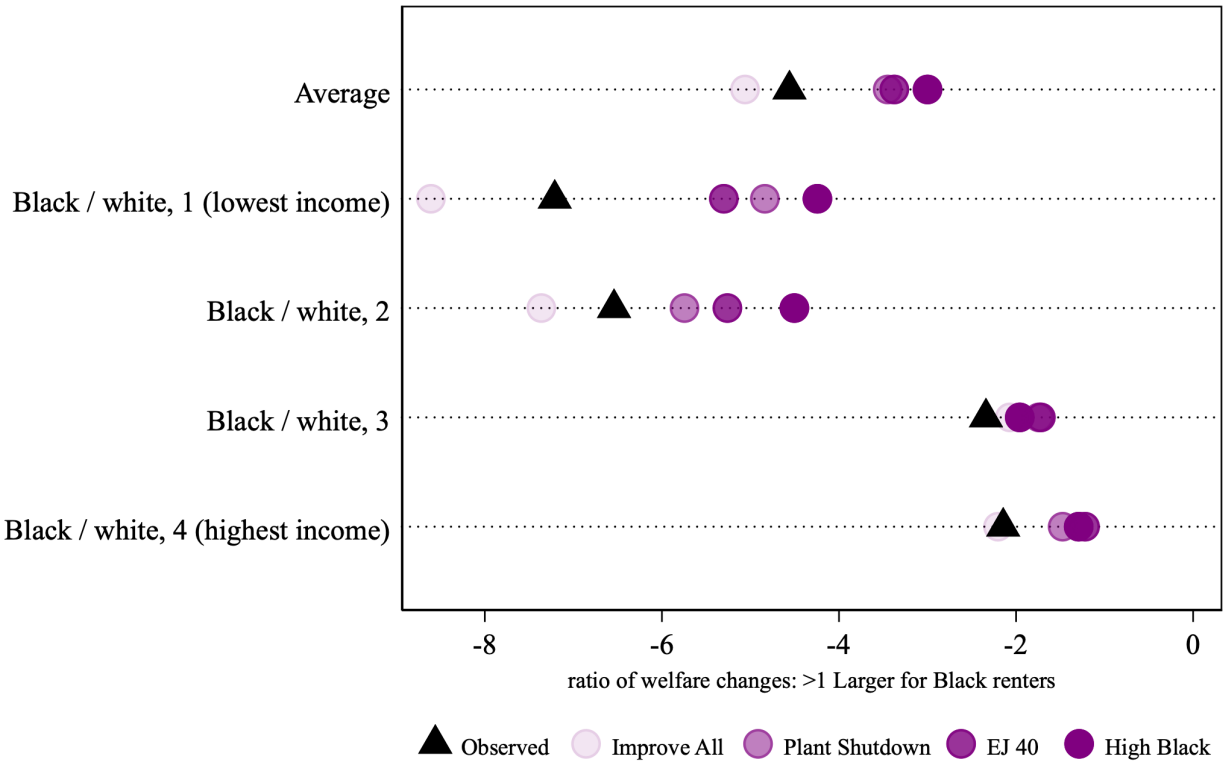
EJ 40 | Plant Shutdown

NOTES: This figure shows the estimated changes in $\widehat{\delta_{jt}}$ associated with each counterfactual due to the simulated air quality changes.

groups.

Many environmental justice policies and empirical environmental justice research focuses on pollution as the key outcome of interest, and so we also compute pollution outcomes in a general and partial equilibrium framework. In the general equilibrium framework, we compute pollution outcomes by race using our estimates of equilibrium race shares under the counterfactual air quality simulations and 2018 air quality, together with a metric of population weighted pollution. Our population-weighted pollution metric multiplies air quality—concentrations of $PM_{2.5}$—in a census tract by the total number of renters of a given race group in that census tract, divided by the total population of renters of that race in the Chicago CBSA. In sum, our population-weighted pollution metric in our partial requilibrium

Figure 7: Welfare change ratios by income type and scenario



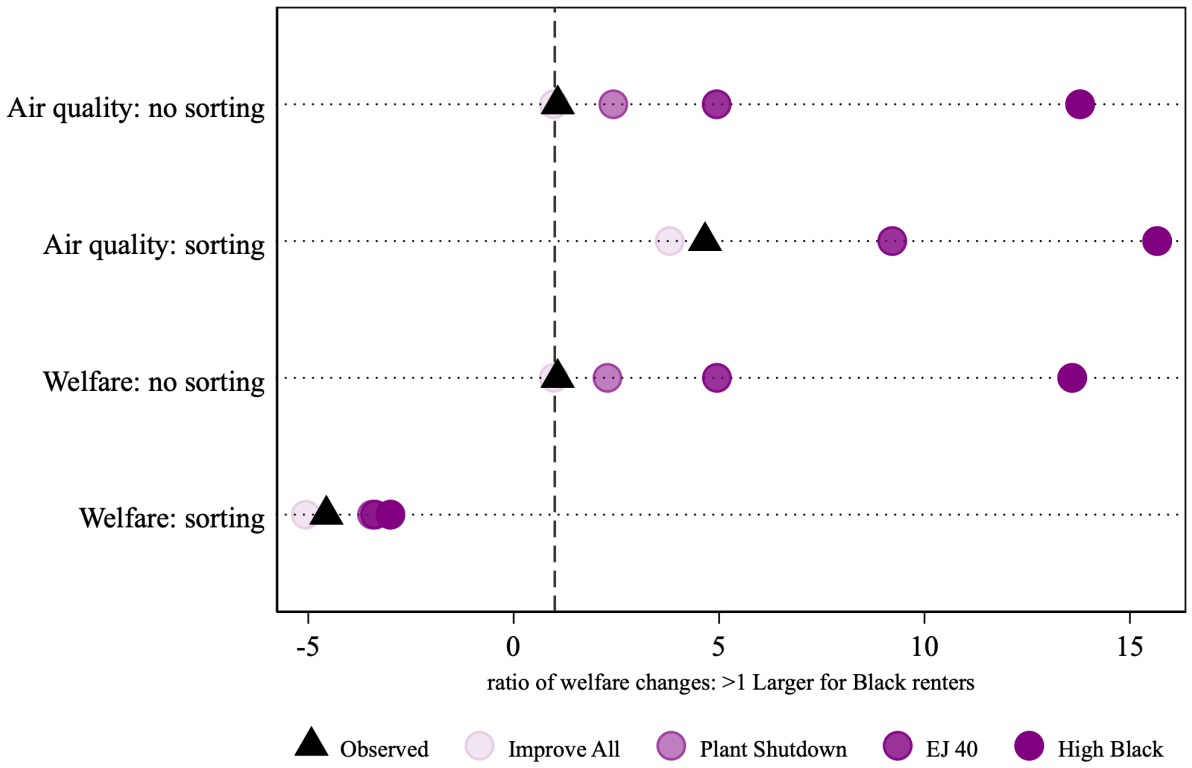
NOTES: The figure plots the ratio of expected welfare from equation (3) constructed with our parameter estimates by income type in the observed and counterfactual scenarios, with an additional contraction mapping to find equilibrium race shares.

approach represents pollution changes with no migration; while this metric in the general equilibrium approach includes migration.

The welfare and pollution ratios in the partial (no sorting model) and general (sorting model) equilibrium frameworks are shown in Figure 8. The top two rows show the ratio of population weighted pollution changes for Black versus white renters, averaged over all income types, and the lower two rows show welfare ratios. The first and third rows show the results for each metric computed in a partial equilibrium approach, and the second and fourth rows show the results in a general equilibrium framework. We multiply pollution reductions from state x_0 to x_1 by -1 so that improvements are positive values. For all simulations in general and partial equilibrium, both Black and white renters see pollution reductions, except for the *Plant Shutdown* simulation in general equilibrium, where white renters see an increase in pollution. This increase in pollution in this simulation—negative value in the denominator—changes the interpretation of r_{BW} for this simulation. To facilitate visual comparability, this ratio is excluded from the figure; though the takeaway is clear—pollution disparities are narrowed in this simulation in general equilibrium.

The first two rows of Figure 8 show that Black-white pollution disparities narrow in all simulations in both general (sorting model) and partial equilibrium (no sorting model) frameworks. Interestingly, the narrowing is attenuated in the no sorting framework. That is, when incorporating sorting responses to the policy, the simulations generate larger reductions in Black-white pollution disparities compared to when sorting is not accounted for. In both modeling approaches, the *High Black* simulation leads to the largest reduction in Black-white pollution disparities. The fourth row represents the results from Figure 7 averaged over income type. Comparing row two to row four, we find that in a general equilibrium framework, policies can generate reductions in pollution disparities while widening welfare disparities. These findings are particularly important in the context of policy decision-making. A policy making proceeding would typically use an estimate of MWTP for pollution reduction as input to a cost-benefit analysis. We show that this approach would not only overestimate the benefits of a pollution reduction but would predict the opposite sign in terms of welfare inequality: the partial equilibrium analysis predicts that these policies are welfare narrowing, while the general equilibrium analysis predicts that they are welfare widening.

Figure 8: Expected welfare and air quality change ratios in sorting model (general equilibrium) vs. no sorting (partial equilibrium) approaches



NOTES: The figure plots the ratio of air quality changes and expected welfare from two approaches shown in different rows. Air quality change ratios are constructed by computing renter population weighted pollution. Welfare change ratios in the sorting row are constructed according to equation (3), with an additional contraction mapping to find equilibrium race shares. Welfare changes in the no sorting row assume that renters benefit from air quality improvements in their residential location in an amount equal to Grainger (2012)'s marginal willingness to pay estimate for pollution improvement.

Environmental justice criteria often use pollution as the outcome of interest. Our general equilibrium framework predicts that all policies narrow Black-white pollution inequalities.

6 Conclusion

This paper develops a new approach for accounting for endogenous amenities in sorting models. This method is applicable to a broad range of research questions studying the welfare impacts of amenity changes. Provided the researcher has a source of exogenous variation, our approach is straightforward to implement and does not require observations of indirectly affected amenities nor functional form assumptions around indirect effects. In addition, we

apply a novel measure of expected welfare that emerges from our discrete choice model to characterize racial inequality. Much of the environmental justice literature in economics to date focuses on documenting gaps in pollution, with less focus on welfare (Cain et al., 2024). The welfare ratio metric we use offers a path for more empirical work to document not just changes in pollution gaps, but also in welfare.

Our empirical findings have two main takeaways. First, a place-based policy that improves local air quality may reduce pollution disparities, while at the same time widening welfare disparities. Second, using a partial equilibrium framework to estimate the impacts of place-based clean-up on welfare inequality in a partial equilibrium framework can lead to the opposite conclusion about the ability of a policy to lower welfare inequality. This is a cautionary tale for cost-benefit analyses that use marginal willingness to pay estimates to approximate the value of an amenity improvement.

It is important to caveat that our results describe the outcomes for renters and are not applicable to home owners. The incentives for renters are different from those of owners, who have the ability to capitalize local amenity improvements but introduce new forms of moving costs and forward looking expectations (Bayer et al., 2016). Studying similar questions with respect to owners is an excellent topic for future work.

References

Bakkensen, Laura A, and Lala Ma. 2020. "Sorting over flood risk and implications for policy reform." *Journal of Environmental Economics and Management*, 104: 102362.

Banzhaf, Spencer, Lala Ma, and Christopher Timmins. 2019. "Environmental Justice: The Economics of Race, Place, and Pollution." *Journal of Economic Perspectives*, 33(1): 185–208.

Bartik, Alexander W, Janet Currie, Michael Greenstone, and Christopher R Knittel. 2019. "The local economic and welfare consequences of hydraulic fracturing." *American Economic Journal: Applied Economics*, 11(4): 105–55.

Bayer, Patrick, Fernando Ferreira, and Robert McMillan. 2007. "A unified framework for measuring preferences for schools and neighborhoods." *Journal of political economy*, 115(4): 588–638.

Bayer, Patrick, Robert McMillan, Alvin Murphy, and Christopher Timmins. 2016. "A dynamic model of demand for houses and neighborhoods." *Econometrica*, 84(3): 893–942.

Berry, Steven, James Levinsohn, and Ariel Pakes. 1995. "Your use of the JSTOR archive indicates your acceptance of the Terms & Conditions of Use, available at http://about. jstor. org/terms." *Econometrica*, 63(4): 841–890.

Bondy, Malvina, Sefi Roth, and Lutz Sager. 2020. "Crime is in the air: The contemporaneous relationship between air pollution and crime." *Journal of the Association of Environmental and Resource Economists*, 7(3): 555–585.

Bowen, William. 2002. "An Analytical Review of Environmental Justice Research: What do we Really Know?" *Environmental Management*, 29(1): 3–15.

Bullard, Robert. 2000. *Dumping in Dixie: Race, Class, and Environmental Quality.* Westview Press.

Cain, Lucas, Danae Hernandez-Cortes, Chris Timmins, and Paige Weber. 2024. "Recent Findings and Methodologies in Economics Research in Environmental Justice." *Review of Environmental Economics and Policy.*

Christensen, Peter, and Christopher Timmins. 2022. "Sorting or steering: The effects of housing discrimination on neighborhood choice." *Journal of Political Economy*, 130(8): 2110–2163.

Christensen, Peter, Ignacio Sarmiento-Barbieri, and Christopher Timmins. 2022. "Housing discrimination and the toxics exposure gap in the United States: Evidence from the rental market." *Review of Economics and Statistics*, 104(4): 807–818.

Colmer, Jonathan, Ralf Martin, Mirabelle Muûls, Ulrich J Wagner, et al. 2020. "Does pricing carbon mitigate climate change? Firm-level evidence from the European Union emissions trading scheme." *Center for Economic Performance Discussion Paper*, , (1728).

Currie, Janet, Eric A Hanushek, E Megan Kahn, Matthew Neidell, and Steven G Rivkin. 2009. "Does pollution increase school absences?" *The Review of Economics and Statistics*, 91(4): 682–694.

Currie, Janet, John Voorheis, and Reed Walker. 2020. "What Caused Racial Disparities in Particulate Exposure to Fall? New Evidence from the Clean Air Act and Satellite-Based Measures of Air Quality." National Bureau of Economic Research Working Paper 26659.

Davis, Morris A, Jesse Gregory, and Daniel A Hartley. 2023. "Preferences over the racial composition of neighborhoods: Estimates and implications." *Available at SSRN 4495735*.

Depro, Brooks, Christopher Timmins, and Maggie O'Neil. 2015. "White Flight and Coming to the Nuisance: Can Residential Mobility Explain Environmental Injustice?" *Journal of the Association of Environmental and Resource Economists*, 2(3): 439–468.

Diamond, Rebecca. 2017. "Housing supply elasticity and rent extraction by state and local governments." *American Economic Journal: Economic Policy*, 9(1): 74–111.

Goodkind, Andrew L, Christopher W Tessum, JS Coggings, Jason D Hill, and Julian D Marshall. 2019. "InMAP source-receptor matrix (ISRM) dataset."

Grainger, Corbett A. 2012. "The distributional effects of pollution regulations: Do renters fully pay for cleaner air?" *Journal of Public Economics*, 96(9-10): 840–852.

Hausman, Catherine, and Ryan Kellogg. 2015. "Welfare and distributional implications of shale gas." National Bureau of Economic Research.

Hausman, Catherine, and Samuel Stolper. 2021. "Inequality, information failures, and air pollution." *Journal of Environmental Economics and Management*, 110: 102552.

Heblich, Stephan, Alex Trew, and Yanos Zylberberg. 2021. "East-side story: Historical pollution and persistent neighborhood sorting." *Journal of Political Economy*, 129(5): 1508–1552.

Hernandez-Cortes, Danae, Kyle C Meng, and Paige Weber. 2023. "Decomposing Trends in US Air Pollution Disparities from Electricity." *Environmental and Energy Policy and the Economy*, 4(1): 91–124.

Herrnstadt, Evan, and Erich Muehlegger. 2015. "Air pollution and criminal activity: Evidence from Chicago microdata." National Bureau of economic research.

Jacobsen, Grant D. 2019. "Who wins in an energy boom? Evidence from wage rates and housing." *Economic Inquiry*, 57(1): 9–32.

Kuminoff, Nicolai V, V Kerry Smith, and Christopher Timmins. 2013. "The new economics of equilibrium sorting and policy evaluation using housing markets." *Journal of economic literature*, 51(4): 1007–1062.

Liang, Yuanning, Ivan Rudik, Eric Yongchen Zou, Alison Johnston, Amanda D Rodewald, and Catherine L Kling. 2020. "Conservation cobenefits from air pollution regulation: Evidence from birds." *Proceedings of the National Academy of Sciences*, 117(49): 30900–30906.

Liu, Haoming, and Alberto Salvo. 2018. "Severe air pollution and child absences when schools and parents respond." *Journal of Environmental Economics and Management*, 92: 300–330.

Liu, Zhaoyang, Nick Hanley, and Danny Campbell. 2020. "Linking urban air pollution with residents' willingness to pay for greenspace: A choice experiment study in Beijing." *Journal of Environmental Economics and Management*, 104: 102383.

Meng, Jun, Chi Li, Randall V Martin, Aaron van Donkelaar, Perry Hystad, and Michael Brauer. 2019. "Estimated long-term (1981–2016) concentrations of ambient fine particulate matter across North America from chemical transport modeling, satellite remote sensing, and ground-based measurements." *Environmental science & technology*, 53(9): 5071–5079.

Mohai, Paul, David Pellow, and J. Timmons Roberts. 2009*a*. "Environmental Justice." *Annual Review of Environment and Resources*, 34(1): 405–430.

Mohai, Paul, David Pellow, and J Timmons Roberts. 2009*b*. "Environmental justice." *Annual review of environment and resources*, 34: 405–430.

Persico, Claudia, David Figlio, and Jeffrey Roth. 2020. "The developmental consequences of superfund sites." *Journal of Labor Economics*, 38(4): 1055–1097.

Ringquist, Evan J. 2005. "Assessing Evidence of Environmental Inequities: A Meta-analysis." *Journal of Policy Analysis and Management*, 24(2): 223–247.

Rosen, Sherwin. 1974. "Hedonic prices and implicit markets: product differentiation in pure competition." *Journal of political economy*, 82(1): 34–55.

Shen, Siyuan, Chi Li, Aaron van Donkelaar, Nathan Jacobs, Chenguang Wang, and Randall V Martin. 2024. "Enhancing Global Estimation of Fine Particulate Matter Concentrations by Including Geophysical a Priori Information in Deep Learning." *ACS ES&T Air*, 1(5): 332–345.

Stafford, Tess M. 2015. "Indoor air quality and academic performance." *Journal of Environmental Economics and Management*, 70: 34–50.

Tessum, Christopher W, David A Paolella, Sarah E Chambliss, Joshua S Apte, Jason D Hill, and Julian D Marshall. 2021. "PM2. 5 polluters disproportionately and systemically affect people of color in the United States." *Science advances*, 7(18): eabf4491.

Tessum, Christopher W., Jason D. Hill, and Julian D. Marshall. 2017. "InMAP: A model for air pollution interventions." *PLOS ONE*, 12(4): 1–26.

Tessum, Christopher W., Joshua S. Apte, Andrew L. Goodkind, Nicholas Z. Muller, Kimberley A. Mullins, David A. Paolella, Stephen Polasky, Nathaniel P. Springer, Sumil K. Thakrar, Julian D. Marshall, and Jason D. Hill. 2019. "Inequity in consumption of goods and services adds to racial–ethnic disparities in air pollution exposure." *Proceedings of the National Academy of Sciences*, 116(13): 6001–6006.

Train, Kenneth E. 2009. *Discrete choice methods with simulation.* Cambridge university press.

U.S. EIA, The U.S. Energy Information Administration. 2017. "Competition between coal and natural gas affects power markets."

U.S. EIA, U.S. Energy Information Administration. 2018. "Hydraulically fractured horizontal wells account for most new oil and natural gas wells."

Van Donkelaar, Aaron, Melanie S Hammer, Liam Bindle, Michael Brauer, Jeffery R Brook, Michael J Garay, N Christina Hsu, Olga V Kalashnikova, Ralph A Kahn, Colin Lee, et al. 2021. "Monthly global estimates of fine particulate matter and their uncertainty." *Environmental Science & Technology*, 55(22): 15287–15300.

Wang, Wen. 2021. "Environmental Gentrification."

Wang, Xiao, George Deltas, Madhu Khanna, and Xiang Bi. 2021. "Community Pressure and the Spatial Redistribution of Pollution: The Relocation of Toxic-Releasing Facilities." *Journal of the Association of Environmental and Resource Economists*, 8(3): 577–616.

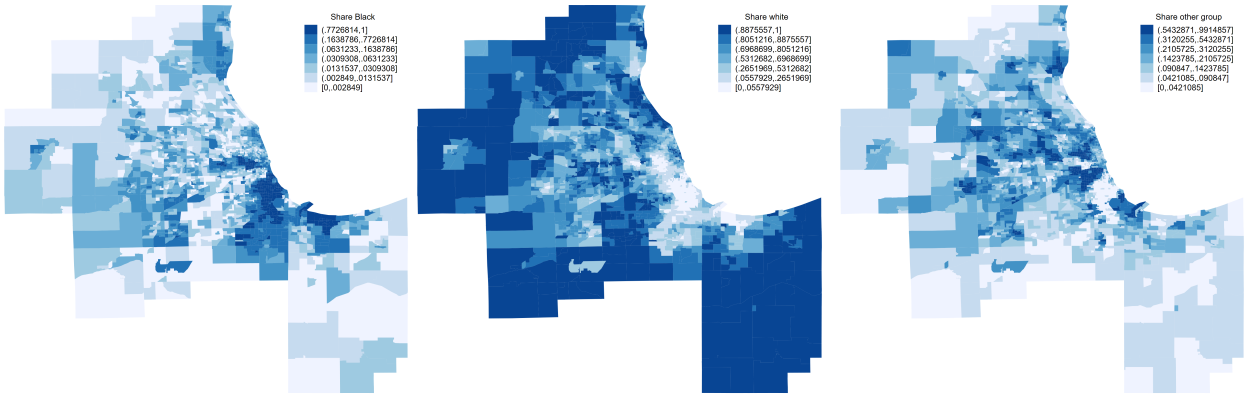
A Appendix: additional descriptives and results

Table A1: Mobility among renters and owners, average 2011–2018 (ACS 5)

	(1) All census tracts	(2) Chicago census tracts
Renters (%)	0.353	0.373
	(0.23)	(0.24)
Owners (%)	0.647	0.627
	(0.23)	(0.24)
Owners - moved from last year (%)	0.071	0.079
	(0.06)	(0.05)
Renters - moved from last year (%)	0.274	0.308
	(0.15)	(0.15)
Owners - moved within same county (%)	0.042	0.036
	(0.04)	(0.04)
Renters - moved within same county (%)	0.168	0.153
	(0.12)	(0.11)
Owners - moved diff. county within same state (%)	0.015	0.026
	(0.02)	(0.03)
Renters - moved diff. county within same state (%)	0.054	0.092
	(0.07)	(0.09)
Owners - moved diff. state (%)	0.011	0.014
	(0.02)	(0.02)
Renters - moved diff. state (%)	0.042	0.054
	(0.06)	(0.07)
Owners - moved from abroad (%)	0.003	0.004
	(0.02)	(0.01)
Renters - moved from abroad (%)	0.009	0.009
	(0.03)	(0.03)
Observations	502302	6620

NOTES: Average mobility among renters and owners in census tracts at the national level (column 1) and in the Chicago CBSA during 2011–2018. TO DO: ADD MOBILITY RATES FROM INFO USA DATA.

Figure A1: Population shares by race



Share Black Share white Share other

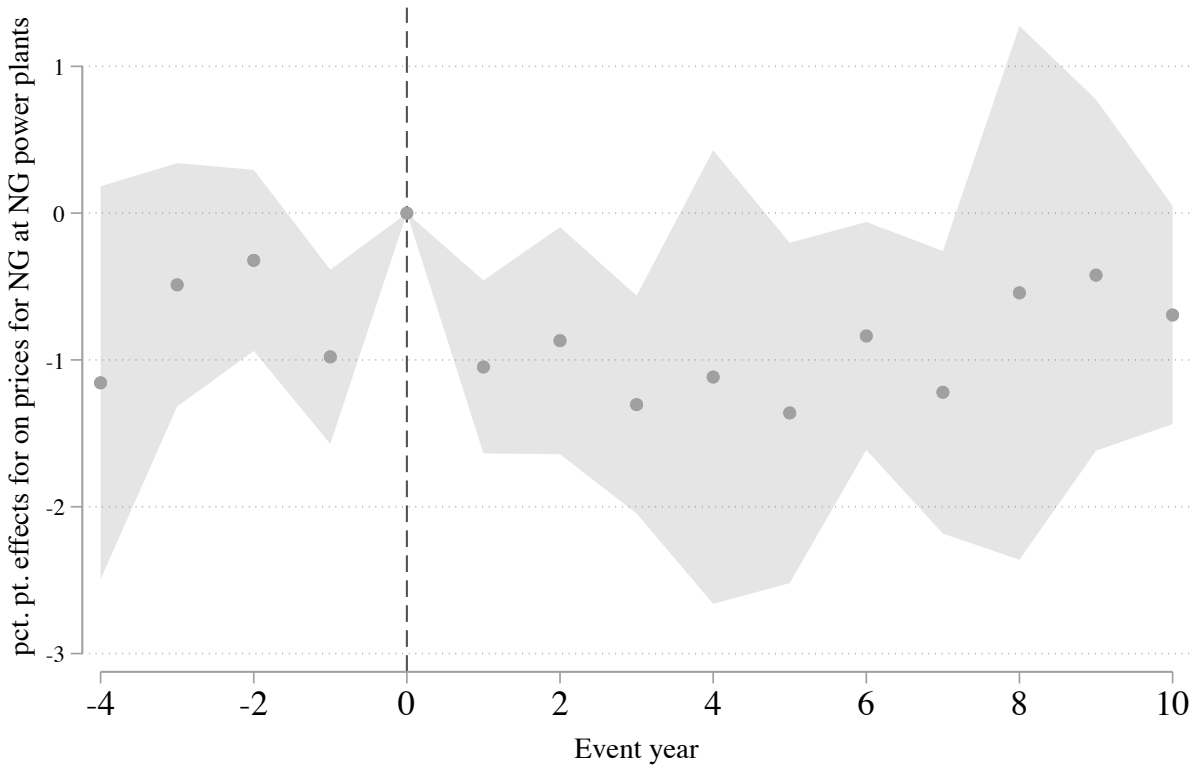
NOTES: Figures show share of different demographic groups in Chicago CBSA.

Table A2: Estimates of marginal willingness to pay (MWTP) for related pollutants in other literature

Paper	Estimate	Units
Chay & Greenstone (2005)	\$2,400	TSP
Bajari, Fruewirth, Kim, & Timmins (2012)	\$54, \$90	ppb SO_2, O_3
Bento, Freedman, & Langer (2015)	\$120-130, \$27	PM_{10}
Bayer, Keohane, & Timmins (2009)	\$165	PM_{10}
Grainger (2012)	\$276	PM_{10}

NOTES: Table shows estimates of marginal willingness to pay for related pollutants from the literature. This list is not intended to be exhaustive and is included for reference. The estimates from the first four papers use housing value as the outcome variable, so can be seen as the MWTP for owners, or renters paying the corresponding monthly rent. Grainger (2012)'s estimate is explicitly for renters, and we use this estimate for the analysis presented in Figure 8.

Figure A2: Event study with fracking-predicted emissions and EIA-923 natural gas prices as dependent variable



NOTES: This figure shows the results from the event study presented in Section 4.3 with plant-level natural gas prices as the dependent variable. Plant-level natural gas prices are obtained from EIA-923 data, which reports plant-level fuel receipts and costs. Since the dependent variable is at the plant and not unit-level, the event study regression here includes plant (not unit) fixed effects. Event year and data year fixed effects are also included.

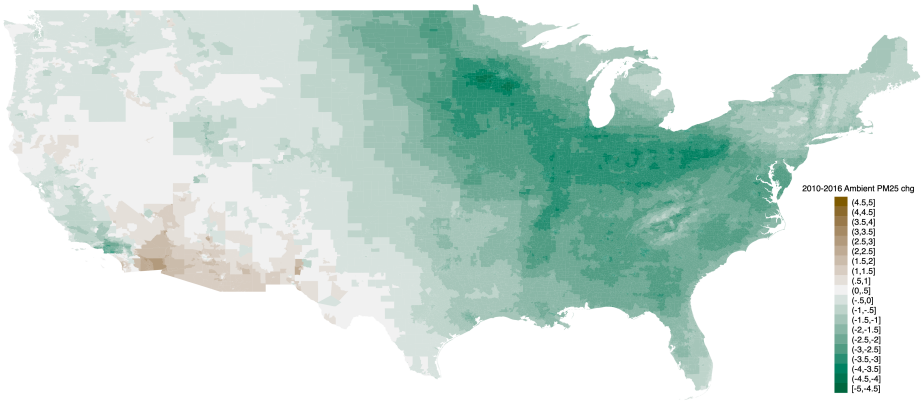
B Appendix: Air quality data

Estimating our model requires time-varying changes in tract-level ambient air quality that are explained by our instrument. This section of the appendix provides further evidence that there is variation in ambient air quality in our study region during our sample period. Appendix C provides additional results related to the instrument used for air quality. We discuss the variation in our air quality data over time and space and corroborate those findings with other data sources.

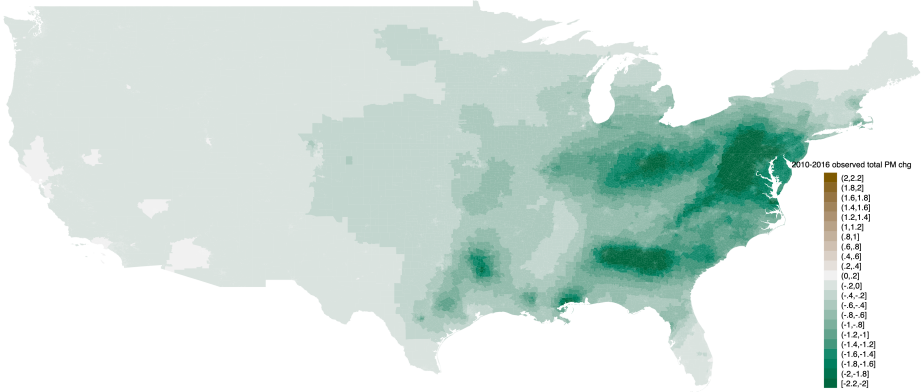
Figure A3 (a) shows the geographic distribution of changes in ambient $PM_{2.5}$ in the United States over 2010–2016 using data from Meng et al. (2019). Figure A3 (b) shows changes in ambient $PM_{2.5}$ generated only from the electricity sector. Hernandez-Cortes, Meng and Weber (2023) demonstrates that coal to gas switching was largely responsible for these reductions.

Figure A3: Changes in $PM_{2.5}$ concentration, 2010–2016

(a) Observed changes in ambient $PM_{2.5}$



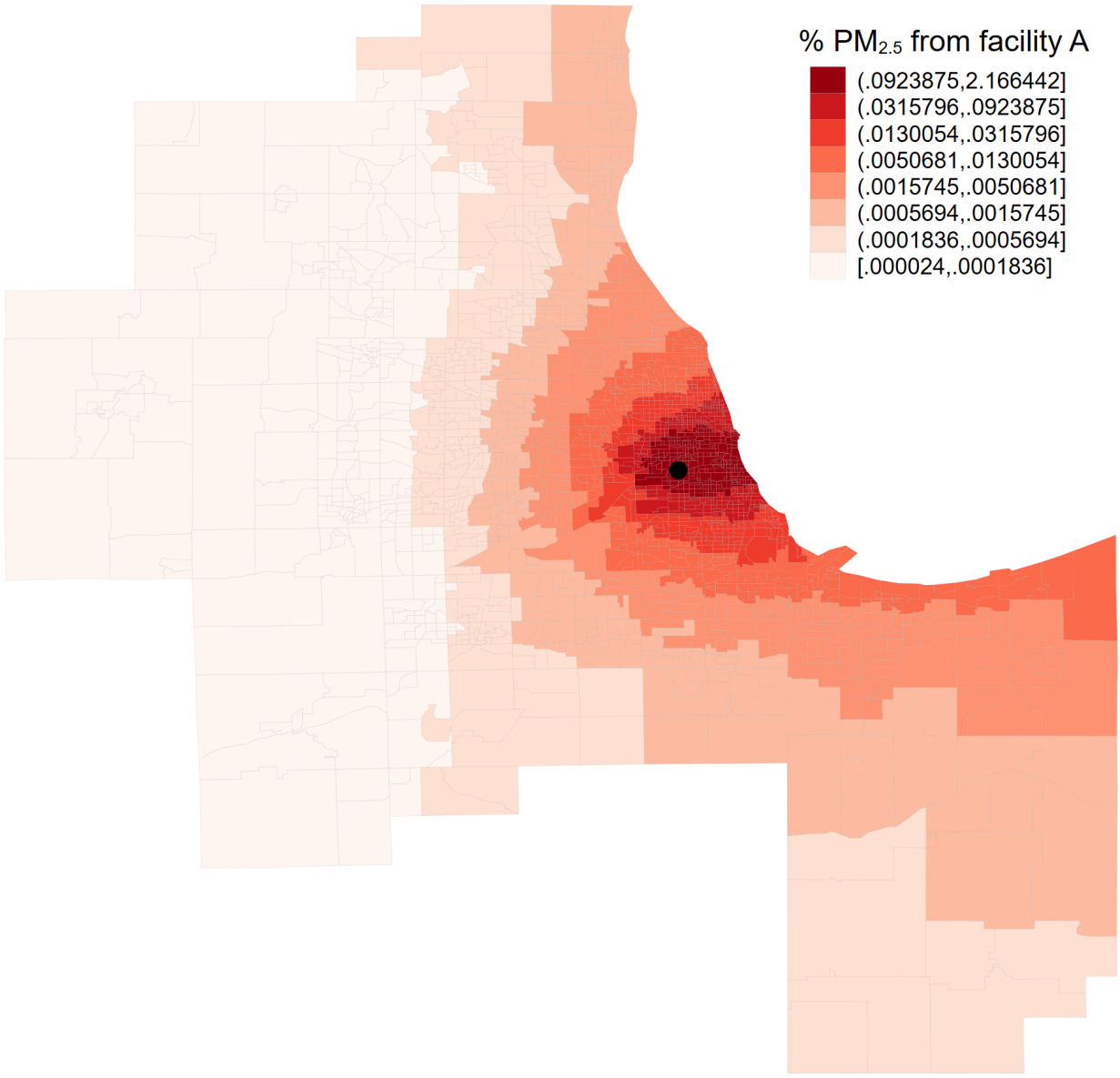
(b) Observed changes in electricity generated $PM_{2.5}$



NOTES: Panel (a) shows the observed changes in ambient $PM_{2.5}$ during 2010–2016 using the (Meng et al., 2019) data. Panel (b) shows the changes in $PM_{2.5}$ concentrations from the electricity generating units in our sample generated by InMAP (Goodkind et al., 2019).

Next we discuss census tract-level variation $PM_{2.5}$ for our empirical setting, the Chicago CBSA. The variation in air quality originates from the location of pollution sources and pollution transport. Electric generating units emit $PM_{2.5}$ precursor pollutants from tall smokestacks. This allows pollution to travel on the basis of physical and chemical processes. These transport patterns create variation in which census tracts receive pollution from the same polluting source. We use InMAP to model these pollution transport patterns. Figure A4 provides an example of the cross-sectional variation provided by the transport patterns from pollutants from a coal-fired electric generating unit located in the Chicago CBSA based on InMAP. In this figure, we modeled a uniform increase of 1000 kg of $PM_{2.5}$ precursors using InMAP. This figure demonstrates that reducing the pollution from one plant would have unique effects on the air quality of different local census tracts. Likewise, reducing emissions from the set of coal units that generate emissions that create pollution for Chicago tracts will create unique patterns of improvement across census tracts.

Figure A4: Pollution concentrations from observed emissions of two facilities in Chicago CBSA

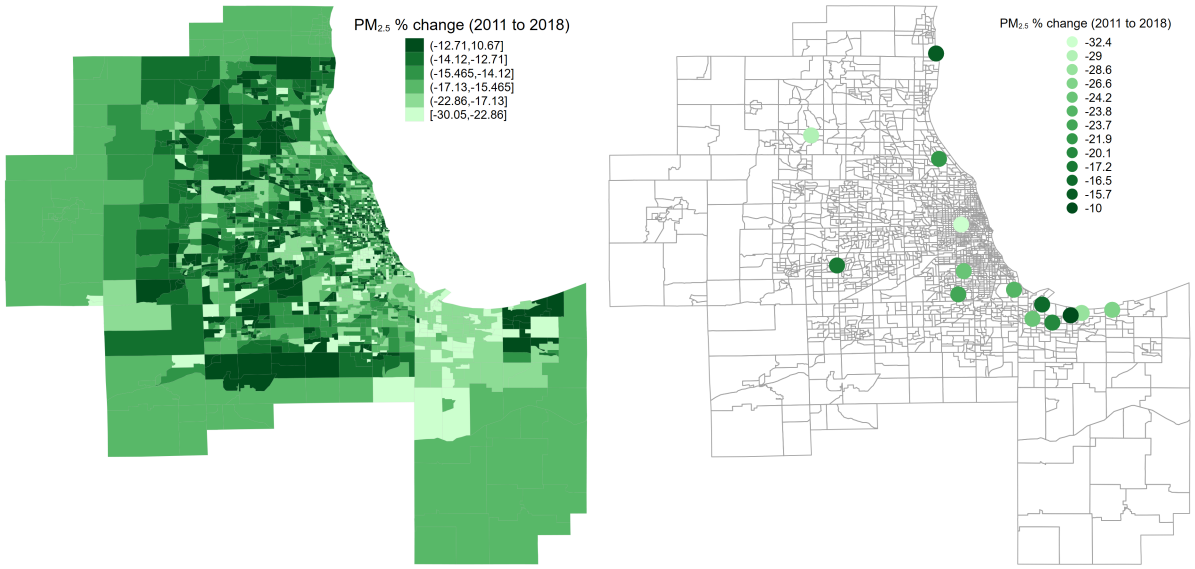


NOTES: Figures show pollution concentrations associated to a coal power plants (ORISPL code: 867) in the Chicago CBSA.

Figure A5 shows the variation in ambient air quality over the study period in the Chicago CBSA using the data from Van Donkelaar et al. (2021), which provides annual $PM_{2.5}$ at a 1km $\times$ 1km resolution. The figure shows that while concentrations of $PM_{2.5}$ reduced for all tracts in the Chicago CBSA over the period 2011–2018, the range of improvement varied from 10–30% reduction in $PM_{2.5}$ in 2018 compared to 2011.

The Van Donkelaar et al. (2021) is a re-analysis data product and as such might include

Figure A5: Changes in $PM_{2.5}$ 2011–2018

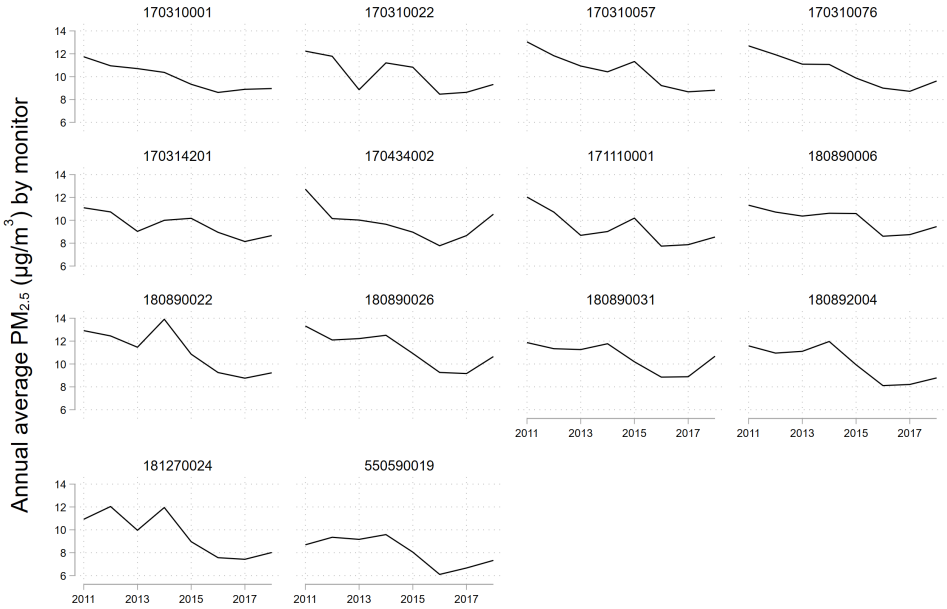


NOTES: Figures show changes in pollution concentrations from the Van Donkelaar et al. (2021) (left) and from EPA monitors (right).

measurement errors. We use hourly $PM_{2.5}$ readings from EPA air quality monitors to study air quality trends during the same period. The monitors have the advantage of providing hourly raw data, and thus potentially less measurement error than re-analysis products, but monitors only provide air pollution readings for distinct points in space, with insufficient geographic coverage for our research question. However, they are useful for comparing time series variation at the monitor locations. Figure A6 plots $PM_{2.5}$ concentrations at the 14 monitors available in the Chicago CBSA during our study period. The average change in the average annual monitor readings for 2018 compared to 2011 was 22 4%. The smallest reduction recorded by a monitor was 10%, while the largest was 32.5%. The results corroborate the time series variation found in the air quality data from Van Donkelaar et al. (2021), which we use in our main analysis.

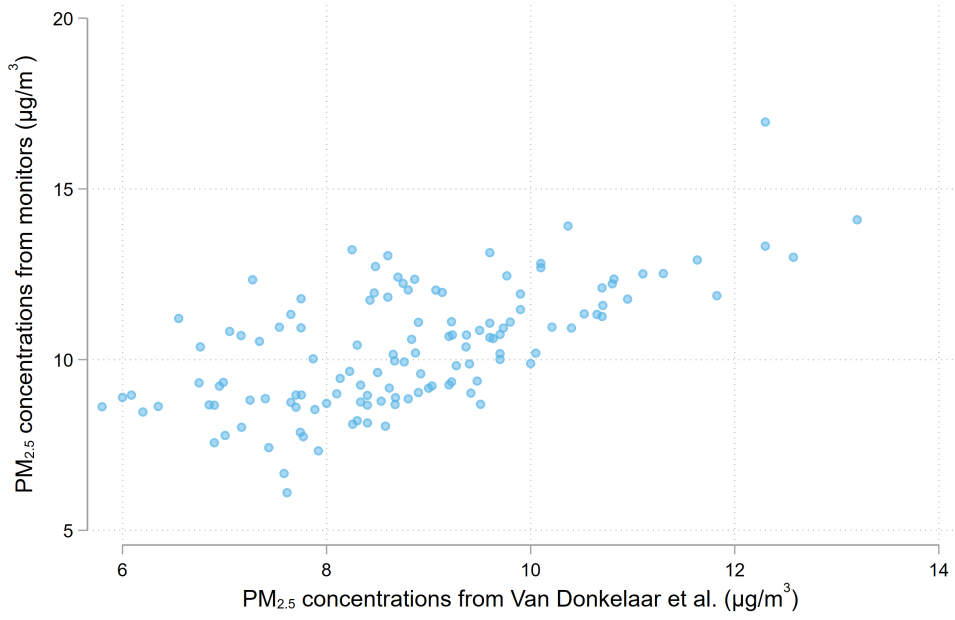
Figure A7 shows the correlation between pollution concentrations from EPA air quality monitors (assigned to the census tract where the monitor is located) and pollution concentrations from Van Donkelaar et al. (2021).

Figure A6: Pollution concentrations trends in Chicago CBSA EPA ambient air quality monitors



NOTES: This figure shows pollution concentrations from 14 pollution monitors in the Chicago CBSA. Each figure represents one pollution monitor's average annual readings from 2010–2018.

Figure A7: Correlation between pollution 2011-2018 concentrations from monitors and Shen et al. (2024)



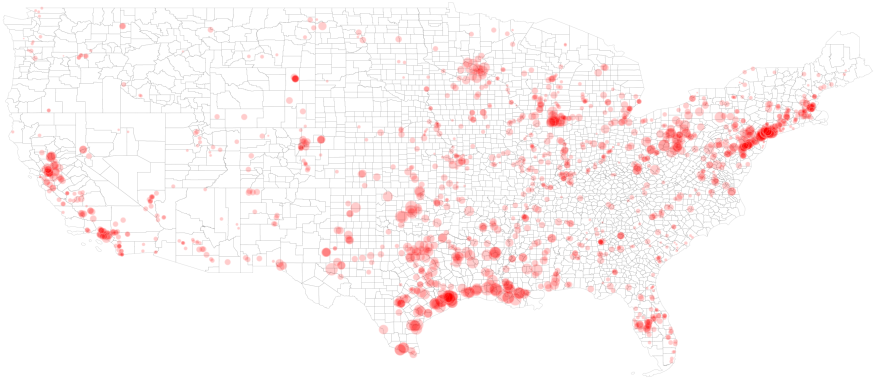
NOTES: This figure shows correlation between pollution concentrations from EPA ambient air quality monitors and satellite data from Van Donkelaar et al. (2021) during 2011-2018.

C Appendix: Air quality instrument

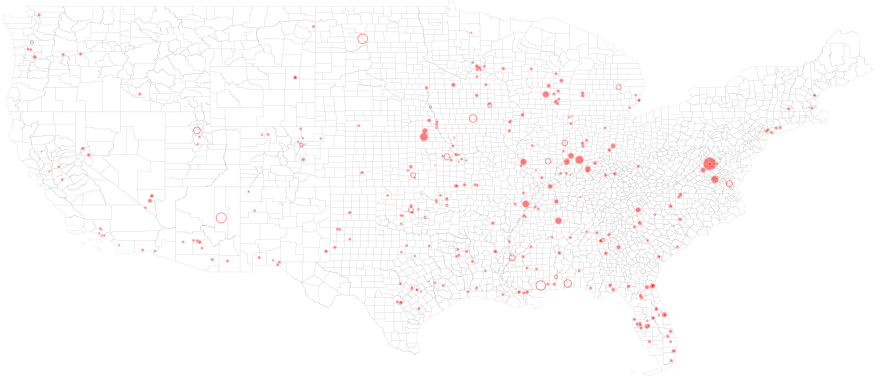
In our main results, we use fracking predicted $PM_{2.5}$ as an instrument for ambient $PM_{2.5}$ in a nonparametric estimation of equation (5). The construction of the instrumental variable is detailed in Section 4.3. Figure A8 shows the geographic variation in S_g, which we use as an instrument for EGU emissions.

Figure A8: Maps supporting the construction of instrument for air quality changes

(a) Generator-level potential natural gas supply from fracking (S_g)



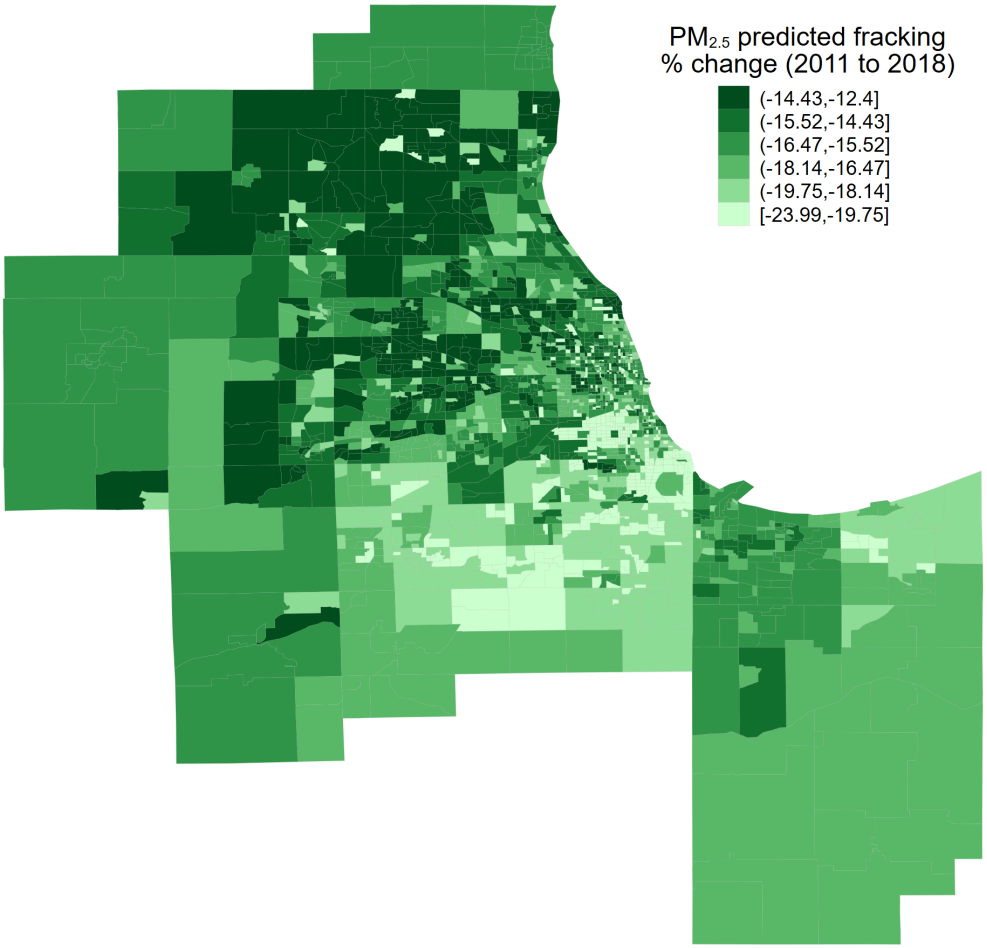
(b) Generator-level changes in observed natural gas prices



NOTES: Panel (a) shows potential fracking supply, defined in the text as the product of prospective fracking score and pipeline density. Panel (b) shows generator-level changes in observed natural gas input prices from EIA Form-923, where solid represents decreases in price change and hollow represents increases in price change.

Table A3 shows the results from the trend-break model estimates from equation (10). Figure A9 shows the changes in air quality predicted by our instrument in the Chicago CBSA. Table A4 reports the estimates from the first stage.

Figure A9: Predicted $PM_{2.5}$ in Chicago CBSA



NOTES: Predicted pollution concentrations changes in the U.S. and Chicago CBSA based on estimation procedure described in Section 4.3.

Table A3: Electricity emissions effects of fracking

	Outcome is (asinh) emissions and concentrations								
	(1)	(2)	(3)	(4)	(5)	(6)	(7)	(8)	(9)
		NO_x			SO_2			$PM_{2.5}$	
post×S_g×ng	13.937		-8.042	18.058		-0.208	13.331		-6.243
	(4.706)		(3.055)	(7.124)		(9.496)	(3.708)		(2.337)
post×S_g×coal	-35.022		-3.891	-34.933		-2.008	-27.385		-2.841
	(9.539)		(5.985)	(10.599)		(9.048)	(7.880)		(4.842)
trend×S_g×ng		-0.762	0.740		1.049	1.089		-0.097	1.069
		(1.191)	(0.927)		(1.747)	(0.666)		(0.823)	(0.730)
post×trend×S_g		4.084	3.092		1.963	1.935		2.961	2.191
×ng		(1.817)	(1.608)		(1.876)	(1.017)		(1.266)	(1.142)
trend×S_g×coal		-1.889	-1.150		-0.071	0.299		-0.641	-0.100
		(1.513)	(1.044)		(1.771)	(0.769)		(1.132)	(0.760)
post×trend×S_g		-4.036	-4.545		-6.619	-6.857		-4.336	-4.710
×coal		(2.261)	(1.967)		(2.225)	(1.669)		(1.784)	(1.558)
Generators	4,922	4,922	4,922	4,922	4,922	4,922	4,922	4,922	4,922
Plants	1,182	1,182	1,182	1,182	1,182	1,182	1,182	1,182	1,182
Counties	691	691	691	691	691	691	691	691	691
Observations	68,604	68,604	68,604	68,604	68,604	68,604	68,604	68,604	68,604

NOTES: This table shows the trend-break model estimates from equation (10). Standard errors in parenthesis, p-values in brackets.

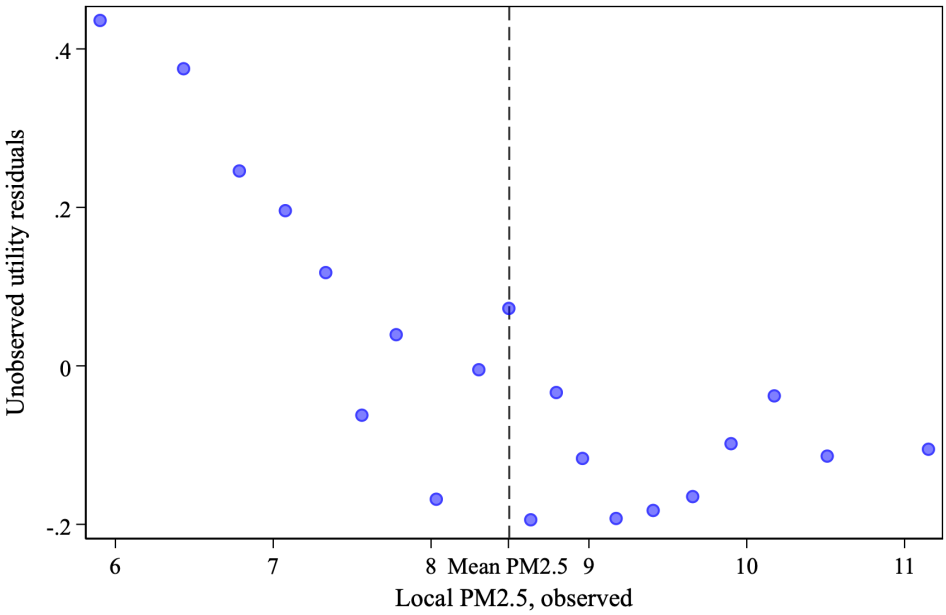
Our objective in estimating equation (5) is to allow location utility to vary flexibly in air quality, which is motivated by Figure A10. This figure plots the de-trended tract-year-income type estimated utility, $\widehat{\delta^{\ell}_{jt}}$, by the observed $PM_{2.5}$ for that tract-year. The de-trending is done by regressing the estimated $\widehat{\delta^{\ell}_{jt}}$ on income, tract, and year fixed effects. We obtain the residuals from that regression and plot them in a binned scatter plot below. Figure A10 shows a nonlinear relationship between the detrended utility and air quality; a linear fitted trend line would have a negative slope, with a lower detrended utility on average among tracts with higher air pollution.

Table A4: First stage of IV: Ambient $PM_{2.5}$ on Fracking-Predicted $PM_{2.5}$, Chicago CBSA 2011–2018

	Ambient $PM_{2.5}$
Predicted PM2.5	0.298***
	(0.000)
Tract FE	Yes
Year FE	Yes
Observations	22100
R-squared	0.958

NOTES: This table shows the results of a regression of tract-year ambient air quality measured in concentration of $PM_{2.5}$ (micrograms per meter cubed). Standard errors in parenthesis. * $p < 0.05$, ** $p < 0.01$, *** $p < 0.001$

Figure A10: Binned scatterplot of unobserved utility residuals on ambient air quality



NOTES: The y-axis are the residuals of a regression of location-year-income type utility estimates from the sorting model on fixed effects for location, year, and income type. These residuals are plotted by location-year air pollution levels on the x-axis. The vertical line shows the average $PM_{2.5}$ in Chicago CBSA over 2011–2018 for reference.

Table A5 presents the Akaike information criterion (AIC) and Bayes information criterion (BIC) for alternative nonparametric functions of equation (5). For this exercise we pool the estimates across income types and include a fixed effect for income type in all regressions. The models each use a natural restricted cubic spline, but vary in the number of knots used in the cubic spline: $\{3, 4, 5\}$; the number of 10km distance bands included in the set z of neighboring census tracts: $\{2, 3, 4, 5, 6\}$, and the function used to measure neighboring

tract distance: Euclidean, exponential, inverse hyperbolic sine, log. As evident in Section 2, we do not directly interpret any of the coefficient estimates of the model to answer our research questions. Rather we use the coefficients to predict unobserved tract-year-income type utility in simulations of counterfactual air quality states. Given these goals, we choose the nonparametric model with the lowest AIC and BIC. Table A5 shows that the model with exponential function of distance, two 10km distance bands of neighbors, and three knots in the cubic spline has the lowest AIC and BIC.

In our sorting model, the term δ_{jt}^{ℓ} includes many factors important to the residential location choice such as housing costs, school quality, and local crime. Here we show our instrument's explanatory power on some of these variables. Table A6 shows the results from several models that regress alternative location amenities on ambient air quality instrumented by fracking predicted air quality. The first column includes log rent prices as the dependent variable, which are obtained from proprietary data provider, Altos. In these data, each rental property-year is an observation in the data set. We observe the zip code of the property but not the census tract, so we match each rental property to the average annual zip code $PM_{2.5}$. To do so, we construct an area-weighted crosswalk of zip codes to census tract polygons, and use that to crosswalk our tract level $PM_{2.5}$, ambient and instrument, to the zip code level.

The tract-level dependent variables in subsequent columns are: (2) police arrests per population; (3) school attendance per population; (4) education spend per student; and (5) graduation rate per enrollment. The arrest data comes from the US FBI's Uniform Crime Reporting program. The data are at the zip code level, and for this analysis, we assume that arrest counts within each zip code are uniformly distributed across the census tract. To calculate an arrest rate per population, the arrest counts at the tract level were divided by the corresponding annual census tract population. School finance data at the school district level is obtained from the Annual Survey of School System Finances conducted by the U.S. Census. These data are available at the district level. We assign each tract the spending of the district in which it is contained. High school-level attendance and graduation rates from annual school report cards are published by the Department of Education for three states within the Chicago CBSA. Illinois, Indiana, and Wisconsin. Data is available at the zip code level, and we assign each tract the attendance and graduation rate for the zip code it is contained in. The availability of school report card data varies by state: Illinois (2010–2019), Indiana (2005–2019), and Wisconsin (2011–2013 and 2015–2018). The regression includes only years in our study period, 2011–2018.

Table A5: AIC and BIC across models of location-utility on instrumented air quality

Distance function	Distance bands	Knots	AIC	BIC	AIC rank	BIC rank
exponential	2	3	321670.9	321707.6	1	1
euclidean	2	3	321672	321708.7	2	2
log	2	3	321672.4	321709.1	3	3
ihs	2	3	321672.4	321709.1	4	4
log	2	4	321678.3	321733.3	5	5
ihs	2	4	321678.4	321733.4	6	6
euclidean	2	4	321678.8	321733.8	7	7
exponential	3	3	321683.9	321738.9	20	8
euclidean	3	4	321679.9	321744	8	9
ihs	3	4	321680.1	321744.3	10	10
log	3	4	321680.1	321744.3	9	11
log	4	3	321680.6	321744.8	11	12
ihs	4	3	321680.7	321744.8	12	13
log	5	3	321680.7	321744.9	13	14
ihs	5	3	321680.8	321744.9	14	15
exponential	2	4	321690.4	321745.4	27	16
euclidean	5	3	321681.8	321746	15	17
euclidean	4	3	321682.2	321746.3	16	18
euclidean	6	3	321682.2	321746.4	17	19
log	6	3	321682.4	321746.6	18	20
ihs	6	3	321682.4	321746.6	19	21
euclidean	2	5	321684.8	321749	21	22
ihs	3	3	321694.2	321749.2	28	23
ihs	4	4	321685.2	321749.3	22	24
log	3	3	321694.4	321749.4	29	25
euclidean	4	4	321685.2	321749.4	24	26
log	4	4	321685.2	321749.4	23	27
log	2	5	321685.2	321749.4	25	28
ihs	2	5	321685.4	321749.5	26	29
euclidean	3	3	321707.3	321762.3	34	30
exponential	3	4	321700.1	321764.3	30	31
ihs	6	4	321706.2	321770.3	31	32
log	6	4	321706.5	321770.6	32	33
ihs	5	4	321707.2	321771.4	33	34
log	5	4	321707.7	321771.8	35	35
euclidean	6	4	321709.5	321773.6	36	36
euclidean	5	4	321716.8	321781	37	37
ihs	3	5	321738.9	321803.1	38	38
log	3	5	321742.1	321806.3	39	39
exponential	2	5	321927.6	321991.8	40	40
exponential	5	3	322219.9	322284.1	42	41
ihs	5	5	322219.9	322284.1	43	42
exponential	5	5	322219.9	322284.1	41	43
exponential	5	4	322219.9	322284.1	44	44
log	5	5	322293.7	322357.9	45	45
euclidean	3	5	322375.9	322440.1	46	46
log	6	5	323784.2	323848.4	47	47
exponential	3	5	323832.9	323897.1	48	48
exponential	6	4	323853.2	323917.3	52	49
ihs	6	5	323853.2	323917.3	51	50
exponential	6	5	323853.2	323917.3	50	51
exponential	6	3	323853.2	323917.3	49	52
exponential	4	3	323958.8	324022.9	53	53
exponential	4	5	323958.8	324022.9	54	54
exponential	4	4	323958.8	324022.9	56	55
ihs	4	5	323958.8	324022.9	55	56
log	4	5	324265.6	324329.8	57	57
euclidean	6	5	324387.6	324451.8	58	58
euclidean	5	5	333090.1	333154.2	59	59
euclidean	4	5	483522.3	483586.5	60	60

NOTES: This table reports the AIC and BIC values across different non-parametric estimates of equation (12), which regresses estimate of location utility by year and income type on an instrument for air quality, including tract and year fixed effects.

Table A6: Amenities on (quadratic) ambient air quality IV: fracking-predicted $PM_{2.5}$

	(1)	(2)	(3)	(4)	(5)
	Log rent	Arrest	Attendence	Eduation spend	Graduation
Ambient $PM_{2.5}$	-0.0515***	-1211.6	-6.343***	3.987	-17.97***
	(-2.902)	(-0.750)	(-11.08)	(0.738)	(-4.798)
Ambient $PM_{2.5}$ sq.	0.0105***	109.0	0.133***	-0.234	0.383
	(9.916)	(0.844)	(3.854)	(-0.539)	(1.566)
Zip	Yes				
Tract		Yes	Yes	Yes	Yes
Year	Yes	Yes	Yes	Yes	Yes
Property attributes	Yes				
Observations	6586547	21336	18291	22100	15291
R-squared	0.246	-4.939	-2.888	-0.188	-0.187

NOTES: T-stats are shown in parenthesis. $^{*}p < 0.1;^{**}p < 0.05;^{***}p < 0.001$. Rental property attributes include binary indicators for the availability of on street parking, off street parking, and garage, pool, fitness center, as well as the number of bedrooms and whether pets are allowed.

D Appendix: Alternative instrument for air quality

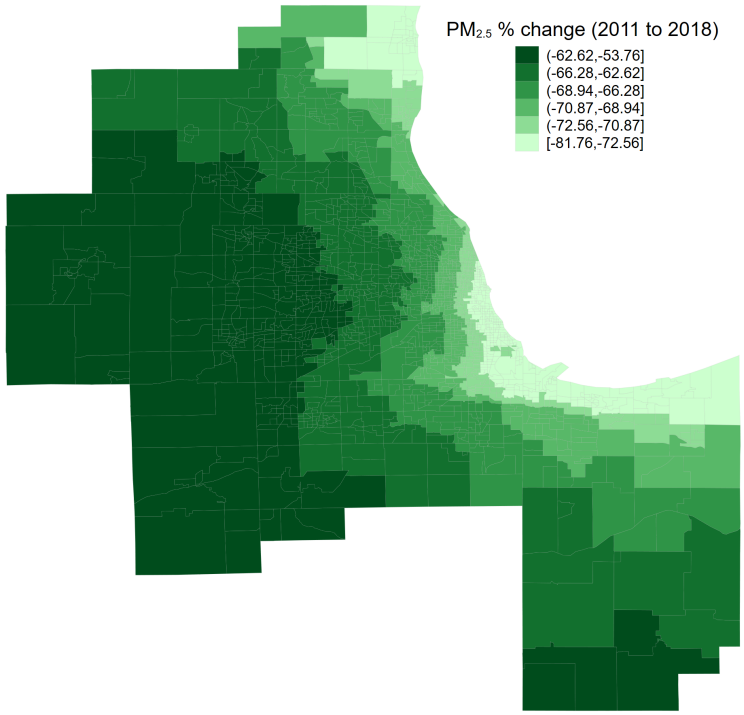
In this section, we discuss another plausibly exogenous source of air quality changes, $PM_{2.5}$ generated by emissions from electricity generating units outside of the Chicago CBSA. To satisfy the exclusion restriction in this setting, it must be the case that time-varying $PM_{2.5}$ generated from emissions from any particular generating unit are unrelated to time-varying components of the error term in equation (12). Since our pollution transport matrix is time invariant, and equation (12) includes tract fixed effects, the exclusion restriction can be discussed in terms of emissions from power plants and their relationship with time-varying components of the error term in equation (12).

If our estimating equation were at the county or state level, it may be plausible that time-varying components of location utility in the error term impact both utility and electricity demand. Local economic growth that adds retail stores could improve local utility while increasing emissions from generating units that increase production to meet this demand. In this setting, however, even this issue would be somewhat mitigated by the fact that economic growth is not likely to systematically increase emissions from upwind as opposed to downwind facilities. However, this type of channel is not likely relevant for an estimation at the census tract level. At this small geographic scale, it is unlikely that local factors that affect the utility of the tract are systematically correlated with time-varying factors that affect emissions in upwind facilities. However, increasing or decreasing emissions from generating units in the Chicago CBSA would be more likely to have very local effects, for example, due to heavier pollutants with smaller dispersal patterns, and thus for this instrument we remove the two electricity generating units located in the CBSA.

We rerun our analysis in this main text with electricity generated $PM_{2.5}$ as our instrument, henceforth, our electricity instrument. The construction of this instrument follows the procedure in Hernandez-Cortes, Meng and Weber (2023), which describes the data and methods to construct $PM_{2.5}$ concentrations attributable to emissions from electricity generating units. Figure A11 shows air quality changes in Chicago CBSA from 2018 compared to 2011 with our instrument generated with electricity $PM_{2.5}$. Comparing this figure with Figure A9, we see that the electricity instrument generates a more systematic pattern of improvements, increasing from the South-West to the North-East of Chicago. Also, predicted improvements in percent change are much larger.

Figure A12 replicates the main welfare ratio results with this instrument. As with our main results, mean welfare change ratios for all policies are less than one, indicating that the policies widen black-white inequality. Both these results are our main results indicate that air quality improvements widen welfare inequality. And our estimated ratios have

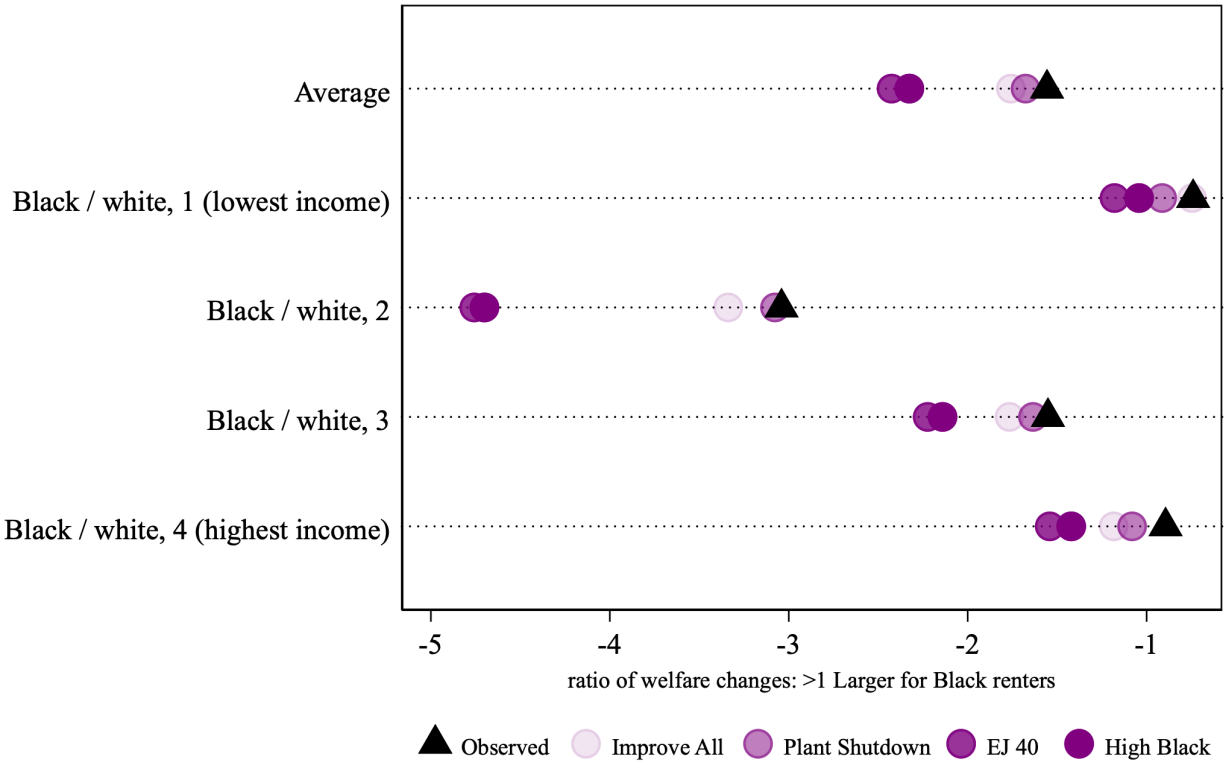
Figure A11: Changes in predicted $PM_{2.5}$ from electricity generation



NOTES: This figure plots changes in ambient $PM_{2.5}$ from 2018 to 2011 using the annual $PM_{2.5}$ predicted from our electricity $PM_{2.5}$ instrument.

comparable magnitudes. However, our preferred instrument for ambient air quality is the fracking instrument, as it requires weaker assumptions to satisfy the exclusion restriction.

Figure A12: Welfare change ratios by income type scenario: Electricity instrument



NOTES: The figure plots the ratio of expected welfare from equation (3) constructed with our parameter estimates by income type in the observed and counterfactual scenarios, with an additional contraction mapping to find equilibrium race shares. This figure use electricity generated $PM_{2.5}$ as an instrument for air quality; the analogous results in Figure 7 use fracking predicted $PM_{2.5}$.

E Appendix: Long difference version of sorting model

We estimate an alternative version of the sorting model that relaxes the assumption that location utilities re-equilibrate annually from amenity changes. In this version of the model, we assume that it takes the full study period to reach a new equilibrium, and estimate the model based on location choices and air quality in 2011 and 2018. We call this the long difference version of the sorting model. The long difference model estimates how changes in air quality at the end of the study period compared to the beginning change residential renter location decisions and welfare by only using data at the beginning and end of the study period.

In the long-difference model, renters are coded as movers in 2011 if they changed census tracts in 2011 compared to 2010. Movers in 2018 are renters who change tracts in 2018 compared to 2011. This empirical choice introduces a difference in the mover coding at the end of the study period compared to the beginning. An alternative would be to code 2011 movers as anyone who changed tracts in 2011 compared to 7 years prior. We avoid doing this for two reasons. One, our goal with this exercise is to generate a comparable set of results with the main annual version of the model, and so in that respect we do not want to introduce new years outside the study period included in the annual model. Two, the air quality improvements, and those explained by our instrument, are more pronounced during our study period. This mover coding choice impacts our estimate of time invariant moving costs in the long difference sorting model. To the extent that this generates an undercount of movers in 2011 compared to movers in 2018, that would bias moving cost estimates upward in a long difference framework. Note, moving costs across the annual and long difference models should not be compared as each model includes its own unique normalization of location utilities.

Our estimates of welfare change ratios in the long difference version of the model are presented in Figure A13. The ratios in the long difference model on average less than one, with positive numerators and denominators, indicating that the air quality improvements overall are welfare widening. Important to note, conceptually, our partial equilibrium analysis for both the annual and long difference versions of the model would be the same since this analysis modulates 2011 utilities with 2018 air quality. Our annual model is our preferred specification, as it leverages annual variation in location choices and air quality, and it more closely approximates location choices for renters, for which annual leases are highly common.

Figure A13: Welfare ratios in long difference sorting model

